Australian Government
Geoscience Australia

MARINE BIODIVERSITY RESEARCH
Prediction and Management of Australia's Marine Biodiversity

Seabed exposure and ecological disturbance on Australia's continental shelf

Potential surrogates for marine biodiversity

Michael G. Hughes, Peter T. Harris and Brendan P. Brooke

Record
2010/43

GeoCat # 71210

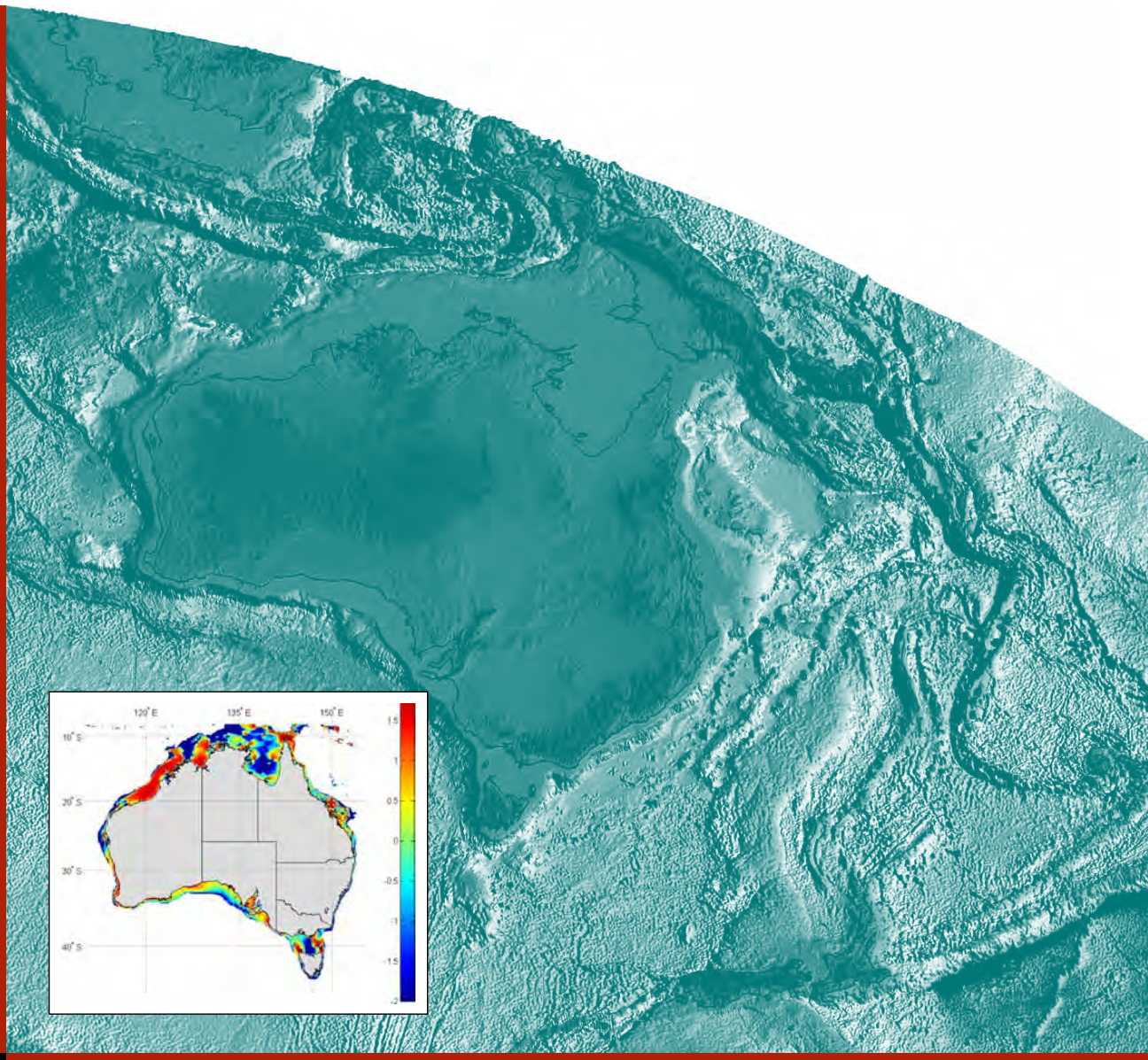

Seabed exposure and ecological disturbance on Australia's continental shelf: Potential surrogates for marine biodiversity

GEOSCIENCE AUSTRALIA
RECORD 2010/43

by

Michael G. Hughes[1], Peter T. Harris[1] and Brendan P. Brooke[1]

Australian Government
Geoscience Australia

MARINE BIODIVERSITY RESEARCH
Prediction and Management of Australia's Marine Biodiversity

1. Marine & Coastal Environment Group, Petroleum & Marine Division, Geoscience Australia, GPO Box 378, Canberra, ACT 2601

Department of Resources, Energy and Tourism
Minister for Resources and Energy: The Hon. Martin Ferguson, AM MP
Secretary: Mr Drew Clarke

Geoscience Australia
Chief Executive Officer: Dr Chris Pigram

ISSN 1448-2177
ISBN 978-1-921781-53-7 (Web)
ISBN 978-1-921781-54-4 (Print)

GeoCat # 71210

Bibliographic reference: Hughes, M.G., Harris, P.T and Brooke, B.P. (2010) Seabed exposure and ecological disturbance on Australia's continental shelf: Potential surrogates for marine biodiversity. Geoscience Australia Record 2010/43, 78pp.

Contents

Executive Summary

Disturbances characterise many natural environments – on land, a forest fire that removes a patch of old-growth trees is an example. The trees that first colonise the vacant patch may be a different species to the surrounding old-growth forest and hence, taken together, the disturbed and undisturbed forest has a higher biodiversity than the original undisturbed forest. This simple example demonstrates the intermediate disturbance hypothesis (IDH) that has applications in many natural environments. The application of IDH is significant for managers tasked with managing and conserving the biodiversity that exists in a given area.

In this report we have used models of seabed sediment mobilisation to examine IDH for Australia's continental shelf environment. Although other disturbance processes may occur (eg. biological, temperature, salinity, anthropogenic, etc.) our study addresses only the physical disturbance of the seabed by waves and currents. Our study has shown that it is feasible to model the frequency and magnitude of seabed disturbance in relation to the dominant energy source (wave-dominated shelf, tide-dominated shelf or tropical cyclone dominated shelf). We focussed our attention on high-energy, patch-clearing events defined as exceeding the Shields parameter value of 0.25. Based on what is known about rates of ecological succession for different substrate types (gravel, sand, mud) we derive maps predicting the spatial distribution of a dimensionless ecological disturbance index (*ED*), given as:

$$ED = FA\frac{ES}{RI}$$

where *ES* is the ecological succession rate for different substrates, *RI* is the recurrence interval of disturbance events and *FA* is the fraction of the frame of reference disturbed. Our maps for the Australian continental shelf shows small patches of *ED*-seafloor distributed around the continent, on both the inner and outer shelf. The patterns are different for wave-dominated (patches on the outer shelf trending parallel to the coast), tide-dominated (patches crossing the middle-shelf trending normal to the coast) and cyclone-dominated (large oval-shaped patches crossing all depths). Only a small portion of the shelf (perhaps ~10%) is characterised by a disturbance regime as defined here. Within these areas, the recurrence interval of disturbance events is comparable to the rate of ecological succession and meets our defined criteria for a disturbance regime. To our knowledge, this is the first time such an analysis has been attempted for any continental shelf on the earth.

Our work demonstrates that there exists a theoretical basis for the existence of disturbance regimes on Australia's continental shelf, which has implications for the protection and conservation of marine biodiversity. Future research is needed to: a) improve modelling of physical processes; b)

measure ecological recovery rates for different habitats; and c) quantify the spatial scales associated with different disturbance processes. Field studies of the spatial scale of physical disturbances caused by storms or intruding ocean currents on continental shelves are lacking and this is a major impediment to linking process studies to the design of spatial marine zone management tools.

Acknowledgements

The authors are grateful for the support and encouragement of our colleagues in the Commonwealth Environment Research Facilities (CERF) Marine Biodiversity Hub. The CERF programme is an Australian Government initiative supporting world class, public good research. Thanks to Anna Potter for assistance with drafting the gravel-sand and mud map of Australia. We are grateful for reviews of an earlier version of this report provided by Dr. Nic Bax (CSIRO and CERF Marine Biodiversity Hub, Hobart) and Dr. Andrea Ogston (University of Washington, Seattle, USA), which improved the content and presentation of the information. This record is published with the permission of the Chief Executive Officer of Geoscience Australia, and the Director of the CERF Marine Biodiversity Hub.

1. Introduction

1.1 MARINE BIODIVERSITY HUB OVERVIEW

The Marine Biodiversity Hub is part of the Commonwealth Environment Research Facilities (CERF) Program administered by the Australian Government's Department of Environment, Heritage, Water and the Arts (DEWHA). The Hub partners are University of Tasmania, CSIRO Wealth from Oceans Flagship (WfO), Geoscience Australia (GA), the Australian Institute of Marine Science and Museum Victoria. The Hub was established in 2007 to undertake research into the prediction and management of patterns of biodiversity in the Australian Marine Estate, especially in support of the Commonwealth Government's Marine Bioregional Planning program. It comprises four multidisciplinary collaborative programs: Biodiversity Patterns, Prediction of Biodiversity, Surrogates of Biodiversity and Off-Reserve Management Options. Descriptions of each program are provided on the Hubs website (http://www.marinehub.org/index.php/site/home/).

1.2 THE SURROGATES PROGRAM

The aim of the Marine Hub's Surrogates Program is to improve our understanding of the ecological processes that link selected environmental variables and patterns in seabed biodiversity, and hence the potential of these variables to act as surrogates of biodiversity. The program comprises three key projects: 1. The establishment of datasets which accurately represent a range of marine biophysical variables; 2. The testing of new surrogates of marine biodiversity patterns, and; 3. An analysis of the influence of continental shelf seabed disturbance created by current and wave induced shear-stress on patterns of benthic biodiversity. The results of the third project are presented in this report.

1.3 REPORT AIMS AND OUTLINE

This report provides a description of the physical oceanography, sedimentology and marine ecology that underlies the development of parameters that represent seabed ecological disturbance regimes. Processes that produce seabed exposure and ecological disturbance are examined; the development of parameters that represent these processes are described; and maps of the Australian continental shelf are provided that display the modelled distribution of the degree of seabed exposure and occurrence of benthic disturbance regimes.

The first aim of this report is to present an argument for the application of physical sedimentology principles to derive potential surrogates for marine biodiversity; through representation of either seabed exposure or ecological disturbance. The second is to provide data grids of these potential surrogates for use in predictive models for marine biodiversity. The argument is developed in

Chapter 2 and is based on the premise that sediment transport and the migration of bedforms have the potential to create patches in the benthos. The key parameter in predicting sediment transport and bedform migration is the bed shear stress exerted by waves and currents. A numerical model is used to hindcast an extended time series of bed shear stress on a spatial grid that covers the continental shelf of Australia. The details of the model are described in Chapter 3. The bed shear stress time series available from the model at each grid location is analysed in terms of its probability distribution. Statistical parameters that describe the bulk of the distribution are argued to represent seabed exposure and are presented in Chapter 4. The spectral properties of the time series are also described. Ecological disturbance depends on a critical threshold magnitude of bed shear stress and the recurrence interval between events that exceed the critical threshold. Disturbance also depends on the benthic community present, which is influenced by the sediment type. An ecological disturbance index is defined in terms of these key factors in Chapter 5 and its spatial pattern is described. Broader implications of the previous two result chapters are discussed in Chapter 6, particularly the potential of the exposure and disturbance parameters presented here as surrogates for marine biodiversity. Limitations of the model data are also discussed. Conclusions follow in Chapter 7.

2. Background

2.1 INTRODUCTION

Australia's marine estate is one of the largest and most diverse in the world. For much of it we have very limited knowledge of the physical environment and major marine ecosystems processes, let alone patterns of biological diversity. The quantification of marine physical environmental variables that are linked to ecological processes that influence the distribution of benthic biodiversity (e.g., species richness; community type) is an essential early step towards better understanding our marine environment and our ability to transform ecosystem-based management theory into practice (eg. Cogan et al., 2009). This is especially the case where these physical variables vary in concert with changes in the distribution of biota and thereby may act as surrogates of patterns of biodiversity. This report addresses the question 'how does seabed disturbance induced by current and wave induced shear-stress influence the pattern of marine biodiversity?'. The question is addressed through a combination of oceanographic modelling, ecological theory and a comparative analysis of seabed disturbance and biological data.

A clear distinction is made herein between seabed (or benthic) exposure and ecological disturbance. Both are relevant to this study and are perhaps, but not necessarily, related. Both may influence marine biodiversity. Seabed exposure is examined here in the absence of any consideration of the benthic community present; only the physical stress exerted on the seabed by waves and currents is considered. If a time series of bed shear stress is available at a particular location, the parameters that describe the bulk of the associated frequency distribution of bed stress represent the seabed exposure. Ecological disturbance on the other hand takes due consideration of the nature of the benthic community present and its response to the magnitude and frequency characteristics of the bed shear stress experienced at a given location. The framework used here for exploring ecological disturbance is the intermediate disturbance hypothesis.

2.2 SEABED EXPOSURE

Exposure to physical processes (specifically waves, currents and sediment transport) can cause the tearing of plants and animals from their places of attachment, sediment mobilisation and the burying of organisms, damage to organisms by abrasion, and indirect stress through limiting light availability (Thomsen et al., 2004; Aller and Todorov, 1997; Cheroske et al., 2000; Carruthers et al., 2002; see also review by Hall, 1994). The level of physical stress in an environment therefore exerts some control on the community present, since the community will only consist of species adapted to the

appropriate levels of physical stress. This has been demonstrated in several studies, where a measure of physical stress has been correlated with particular species or communities. For example, sessile epibenthos species abundance is positively correlated with bed shear stress in Torres Strait (Long et al., 1997), and the variation in occurrence of Anthoza *Turbinara* sp. is increasingly explained by increases in bed shear stress levels in excess of 0.4 Pa (Haywood et al., 2007). This suggests that the simple day-to-day exposure of the seabed to fluid shear by waves, tides, wind- and density-driven circulation may explain some patterns in biodiversity. In this study the *seabed exposure* at a site is simply characterised by some measure that represents the bulk distribution of bed shear stress experienced at that site. Parameters representing benthic exposure will be presented here, but they are not intended to specifically represent *ecological disturbance*, which is a more complex issue.

2.3 ECOLOGICAL DISTURBANCE

2.3.1 Disturbance agents

A fundamental tenet of ecology is that ecosystems and species evolve in response to a particular regime where environmental disturbance can play a significant role in controlling such things as life cycles, food and nutrient supply and habitat availability. A definition of ecological disturbance was provided by Pickett and White (1985) as "any discrete event in time that disrupts ecosystem, community or population structure and changes resources, substrate availability, or the physical environment" (i.e. alters niche opportunities for the species capable of living in a given setting). The agents of ecological disturbance can be many and varied including biotic (e.g. predation, nutrient availability), physical (e.g. wave action, temperature), chemical (e.g. dissolved oxygen, pH), and anthropogenic (e.g. trawling, pollution), to list a few (e.g. Svensson et al., 2007; Proulx and Mazumder, 1998; Sousa, 1984). Each of these examples occur at multiple scales, are often contemporaneous, asynchronous and heterogeneous. These processes play a critical role in the dynamic fluctuation of habitat availability and biotic diversity. This report addresses only the physical, specifically, the bed shear stress exerted by waves and currents and the resulting sediment transport, which cause disturbance through the creation of patches in benthic habitat that are available for opportunistic species to colonise.

2.3.2 Patches

When a disturbance agent creates a patch of open space an ecological succession ensues, with different species arriving over time, until the disturbed patch finally reverts to a mature state

(Connell, 1978). Hence landscapes that are subject to different disturbance agents at different times exhibit a degree of patchiness that relates to past disturbances, their colonisation by opportunists and gradual recovery (Figure 2.1). Hierarchies of patches coexist at multiple scales, created by a range of physical and biological processes (Wu and Loucks, 1995). Patchy landscapes, within a specified frame of reference and length scale, therefore contain greater biodiversity per unit area than either the disturbed or undisturbed habitat alone (Figure 2.1).

The size of patches and the degree of patchiness (number of co-existing patches of different ages) are related to the spatial scale and temporal frequency of the physical disturbance. Consider tropical cyclones as an example. Modelling of shelf currents generated by these events show how cyclonic wind-shear can induce a current field having depth-averaged peak flow speeds of >2 m s^{-1} within ~50 km from the eye of the storm (Hearn and Holloway, 1990; Keen and Slingerland, 1993). Such flows have been shown to mobilise the upper metre of bed sediment on the shelf and to disturb the benthos (Morton, 1988; Gagan et al., 1990; Hubbard, 1992). In the case of reef substrates, Van Woesick et al. (1991) described the effects of 1990 tropical cyclone Ivor on the Great Barrier Reef as including breakage and dislodgement of corals, mass-movements of sediments and debris and the removal of sections of reef matrix. These levels of benthic disturbance and the size of the area over which extreme flow speeds occur suggest a potential patch size of up to 100 km diameter associated with tropical cyclones. Puotinen (2004) examined cyclone track information in the Great Barrier Reef extending from 1910 to 1999 and determined the temporal frequency of cyclones on a 1 degree grid over the Great Barrier Reef. The median frequency ranged from one event every 4-15 years.

While the potential patch size and degree of patchiness can be estimated based on the spatial scale and temporal frequency of the disturbing agent, the actual patch size and degree of patchiness depends on several factors such as the heterogeneity of the substrate type (particularly its shear strength), duration and stationarity of the disturbance event, robustness of the benthic species, and the ratio of disturbance frequency to recovery rate, to name only a few. The large number of factors that need to be considered to determine whether or not a patch has been created makes it extremely difficult to predict the patchiness in any given environment. The agents of disturbance considered here may or may not create a cleared patch of substrate suitable for re-colonisation as shown in Figure 2.1, depending on the intensity of the event in relation to the nature of the benthic community and substrate in question. Communities comprised of fragile benthic animals are disturbed by events that attain a lower bed shear stress than communities of robust animals that have evolved to withstand more energetic conditions. Furthermore, different substrates are more or less susceptible to disturbance depending on hardness, biological and chemical binding, particle size, depth, bed morphology, orientation to flow and a range of other factors (see review by Hall, 1994).

2.3.3 Biodiversity and the Intermediate Disturbance Hypothesis

The *intermediate disturbance hypothesis* (IDH) proposes that habitats exposed to an intermediate level of disturbance will have maximum biodiversity (Figure 2.2). Lower levels of disturbance are associated with less biodiverse habitats dominated by the relatively few species that survived competitive exclusion; whereas higher levels of disturbance are associated with less biodiverse habitats dominated by pioneer species (Connell, 1978; Huston, 1979). Intermediate levels of disturbance of a habitat allow for the greatest diversity of species to exist, in large part through the presence of disturbed patches of varying ages and community succession (Section 2.3.2; Figure 2.1). Patchy landscapes, taken as a whole, contain a greater number of species (greater biodiversity) per unit area than either the disturbed or undisturbed habitat alone (Wu and Loucks, 1995).

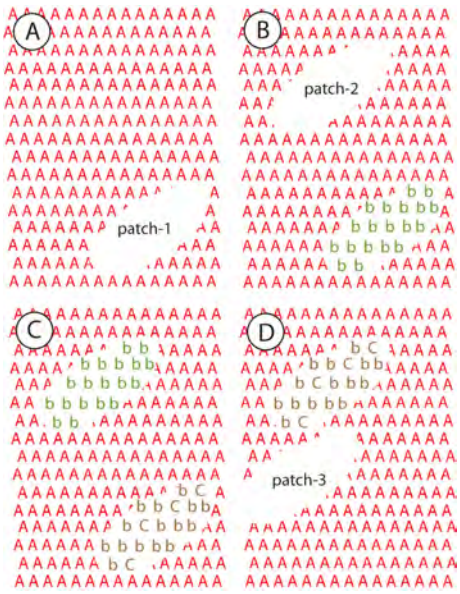

Figure 2.1: *Diagram showing an area of seafloor at four different times, with various disturbed patches of seabed: (A) patch-1 is formed by a disturbance event removing part of community "A"; (B) patch-1 is colonised by early settlers "b" and a second disturbance creates patch-2; (C) patch-1 now supports an intermediate community with members "b" and "C", whereas patch-2 is colonised by early settlers "b"; (D) patch-1 has returned to its original state supporting community "A", patch-2 supports an intermediate community with members "b" and "C" and another disturbance has created patch-3. Biodiversity is greater in B, C, and D because they contain community "A" plus communities "b" and "c", whereas biodiversity is lowest in A, in which only community "A" is present. Note that patch size is dependant upon the scale of the disturbance process; in natural systems, hierarchies of patches are created by asynchronous dynamic processes (from Harris, 2010).*

The IDH predicts that biodiversity is controlled by the frequency of disturbance events, their spatial extent and the amount of time required for ecological succession (Figure 2.2). These factors give rise to patchiness of the seafloor, with coexisting patches at different stages of ecological development (Figure 2.1). After a disturbance, propagules of a few species arrive and settle on the open space. Diversity is low at first, because only the fastest reproducers or species that happen to be located in close proximity can colonise in the short time available. If the frequency of disturbance is too high, then the community will consist only of the few early colonisers (Figure 2.2). With lower disturbance frequencies, the species number will increase with new arrivals until, at some intermediate frequency, a maximum biodiversity is attained (Figure 2.1). If the disturbance frequency is too low, then species numbers are reduced by competition for resources and/or by interference (Connell, 1978; Figure 2.3). Hence an indicator that distinguishes communities that exist in a disturbance regime from other communities is the co-occurrence of habitats in various stages of post-disturbance impact and recovery.

For example, Connell (1978) described how the greatest diversity of corals occurs on the crests of reefs adjacent to Heron Island in the Great Barrier Reef. Reef crests are subject to the full impact of storm events, which destroys the coral and the disturbed areas are colonised by many different coral species. The high species diversity is maintained because colonisation is not so dense that competitive exclusion has reduced the diversity. In contrast, on areas of reef protected from disturbance diversity is reduced by competitive elimination (Connell, 1978; see also Connell, 1997).

In addition to patch-creating processes, the time-scale associated with ecological succession is key to determining whether an intermediate disturbance regime exists. Newell et al (1998) provided a conceptual summary of ecological succession rates typical of temperate estuaries. Recovery periods increased from less than 1 year for muddy substrates, to several years for sandy to gravely substrates and to around 10 years for rocky, reef-type habitats (Figure 2.3). The trend of different recovery times for different substrate types appears to be a consistent pattern among the case studies of ecological successions reviewed by Harris (2010), wherein shorter recovery times of around 1 year relate to soft-sediment habitats and longer recovery times of around 10 years relate to reef habitats. This suggests that the window for the period of disturbance regimes where the IDH could apply should extend from around 1 to 10 years for most shelf benthic communities (Figure 2.3), although this will vary with habitat type and rate of ecological succession.

Field (2005) concluded that “every habitat represents a time-averaged response to the dominant physical processes, which is as important in defining the habitat as geologic setting and community structure.” In seeking suitable surrogates for ecological disturbance on the continental shelf (arising

from physical stress at the seabed) the key questions to resolve are (1) What are the physical shelf processes available to create patches and what is their associated frequency; (2) What is the magnitude of bed shear stress required to create a patch in the benthic community present on an area of shelf; and (3) What is the time-scale associated with ecological succession following patch creation. In the context of the IDH – to maximise biodiversity it is not a sufficient condition to have processes capable of generating large bed shear stresses to create patches, it is also necessary for the frequency of patch generation to be appropriately matched with the time-scale of community succession present. While it is a difficult task to quantify the magnitudes and time-scales related to bed shear stress on the shelf at a national scale it can be approached with data-informed numerical models. To define the nature of the benthic communities present on the shelf at a national scale; their sensitivity to levels of bed shear stress and the time scales of their succession, is an intractable problem! As a consequence, the surrogates proposed in this study to represent *ecological disturbance* will necessarily be based on conjecture informed almost entirely by physical sedimentological principles.

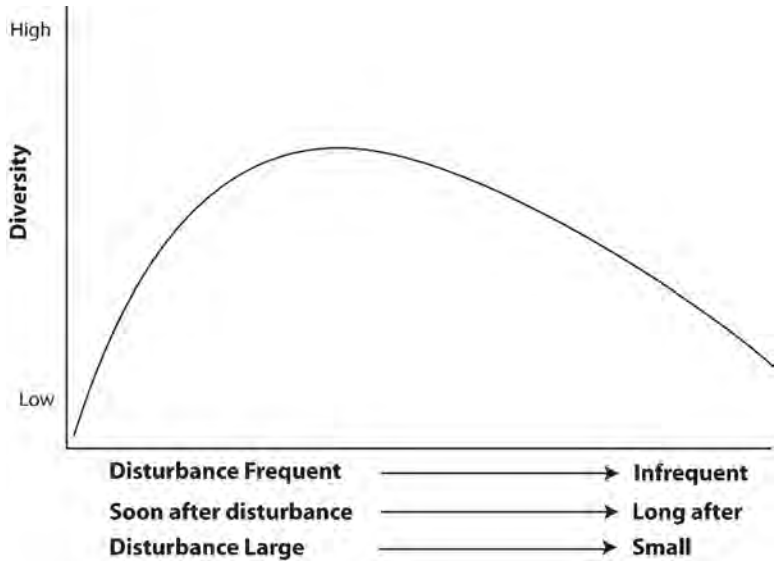

Figure 2.2: *Schematic diagram showing the hypothesised relationship between biodiversity and the frequency of disturbance, elapsed time from disturbance and spatial scale of disturbance (after Connell, 1978). See text for further explanation.*

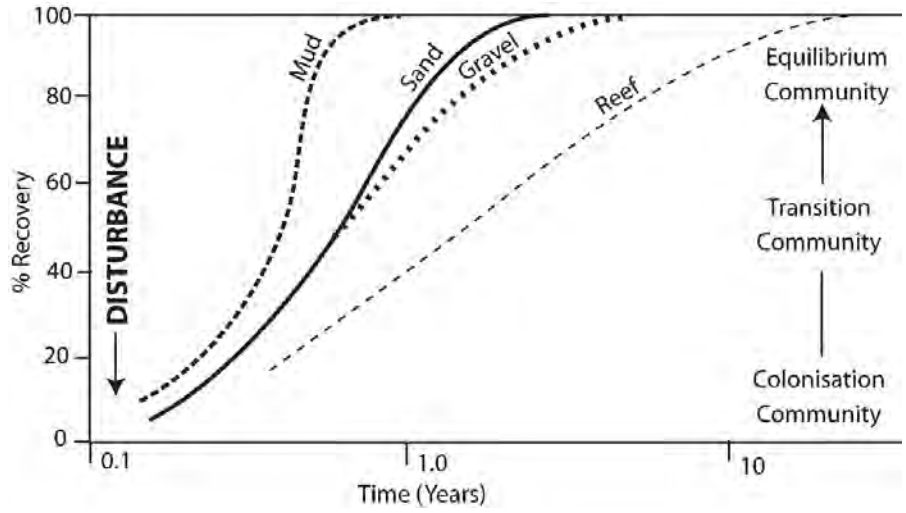

Figure 2.3: *Percentage of recovery for different benthic communities versus time for different substrate types (after Harris, 2010) based on Newell et al., 1998 for gravel sand and mud, with reef recovery times proposed by Done (1992), Harmelin-Vivien (1994) and Halford et al., (2004).*

2.4 PHYSICAL SEDIMENTOLOGY

2.4.1 Sediment entrainment

Sediment transport only begins when the bed shear stress provides sufficient force (lift and drag) to exceed the weight force (gravity) and any cohesive effects acting to stabilise the bed sediment (e.g. Allen, 1985; Nielsen, 1992). This is usually expressed in terms of exceeding the critical bed shear stress required for sediment entrainment (e.g. Sleath, 1984; Soulsby, 1997). The classical work on sediment entrainment was by Shields (1936). He expressed the critical bed shear stress required to initiate sediment motion τ_c, non-dimensionally, as the critical-Shields parameter θ_c

$$\theta_c = \frac{\tau_c}{g(\rho_s - \rho)d} \tag{2.1}$$

where ρ_s is sediment density, ρ is water density and d is grain diameter. We will also refer later to simply the Shields parameter θ, which can be calculated using 2.1 and replacing τ_c with the instantaneous bed shear stress τ, or some statistical representation of it (e.g. the mean or the peak bed shear stress).

Figure 2.4 shows one form of a Shields Diagram, where the critical-Shields parameter θ_c is plotted against the non-dimensional grain diameter D_*

$$D_* = \left[\frac{g(s-1)}{\upsilon^2}\right]^{1/3} d \tag{2.2}$$

(Soulsby, 1997) where g is gravitational acceleration, $s = \rho_s / \rho$ is relative sediment density, and υ is kinematic viscosity of water. Figure 2.4 presents data from measurements under steady currents, waves and combined flows. It shows that for a grain diameter in the medium sand range ($D_* \approx 10 - 20$) the critical Shields parameter $\theta_c \approx 0.05$. The critical Shields parameter increases for coarser sediment, due to the stabilising effect of an increased weight force associated with larger grains. The critical Shields parameter also increases for finer sediment, and this is due to the stabilising effect of grain cohesion (arising from electro-static forces and surface coatings) as well as special boundary layer effects over very fine sediment. The best fit line through the data used to define the onset of sediment transport is described by

$$\theta_c = \frac{0.24}{D_*} + 0.055\left(1 - e^{-0.020 D_*}\right) \tag{2.3}$$

(Soulsby, 1997). To summarise, the occurrence of sediment transport on the continental shelf can be predicted, within a degree of uncertainty reflected by Figure 2.4, from simply knowing the prevailing bed shear stress and sediment grain size.

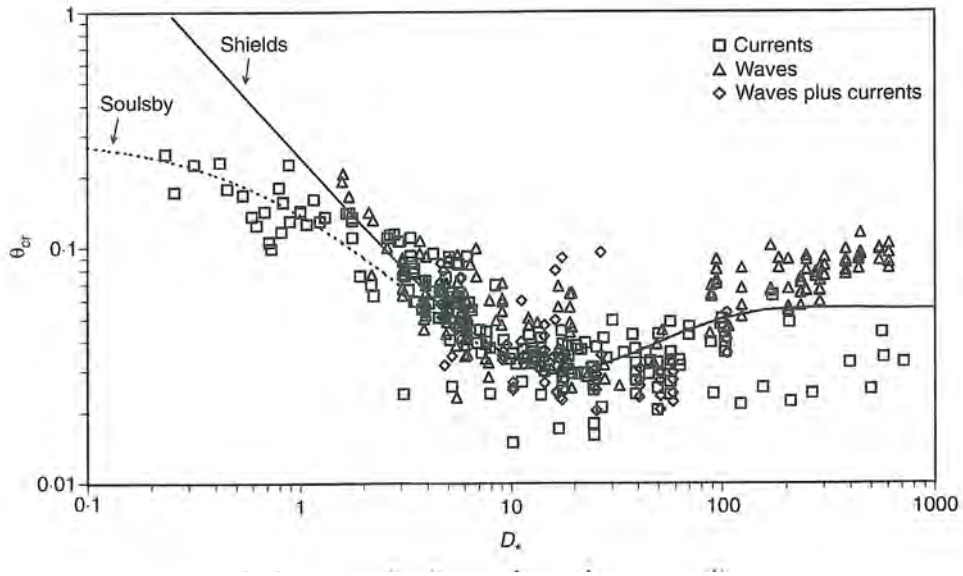

Figure 2.4: *A Shields Diagram used to determine the critical Shields parameter (critical bed shear stress) required to initiate sediment transport. The Shields parameter θ_c is plotted as a function of the non-dimensional grain diameter D_* for available experimental data. For the conditions below the plotted data no sediment transport is expected to occur. The Soulsby curve (dashed line) is described by Equation 2.3 (From Soulsby, 1997).*

2.4.2 Sediment transport

Once in motion, the style or mode of sediment transport is largely determined by the mass of the grain and the speed (and related turbulence intensity) of the current. Sediment transport is usually described by two modes: bed load and suspended load (Figure 2.5).

In the case of bed load, grains are supported by continuous (traction) or intermittent (saltation) contact with the bed (Figure 2.5). In the case of traction, the grains slide or roll along the bed maintaining contact with it at all times. This is a relatively slow form of sediment transport and is typical when relatively weak currents are transporting sands or strong currents are transporting gravels and coarser clasts (Masselink and Hughes, 2003). In the case of saltation, the grains take short hops along the bed, and this mode of transport typically relates to moderate currents transporting sand or strong currents transporting gravels.

In the case of suspended load, grains are supported by the turbulence in the fluid. The grains may make intermittent contact with the bed, but on average they spend most of their time in suspension (Figure 2.5). Suspended sediment transport is typical when moderate currents are transporting silts and clays, or strong currents are transporting sands (Masselink and Hughes, 2003).

The relationship between transport mode and the relative strength of the transporting current, based on laboratory flume experiments, is shown in Figure 2.6. The current strength is expressed in terms of its shear velocity u_*, which is related to the bed shear stress by

$$\tau = \rho u_*^2 \tag{2.4}$$

In Figure 2.6 the shear velocity is non-dimensionalised against the critical shear velocity required for sediment motion u_{*c}. For small values of u_*/u_{*_c} the strength of the current relative to that required to move the sediment available is low and most of the transport occurs as bed load. As u_*/u_{*_c} increases the strength of the current relative to that required to move the sediment becomes larger and suspended load transport becomes increasingly important. The relative strength of the current is determined both by the magnitude of the shear velocity and the size of the available sediment expressed by u_{*c}. For example, a slow current moving over sand is equivalent to a fast current moving gravel, in terms of relative current strength and the associated mode of transport, i.e. bed load. Note that even for very large relative current strengths and high percentages of sediment moving as suspended load, there is always a bed load fraction (Figure 2.6).

Bed load transport, particularly traction, will potentially result in detachment of organisms from the seabed. Saltation and suspended load transport has the potential to impact and damage organisms, as

well as limiting light penetration to the seabed. Persistent sediment transport in both modes can result in the uncovering or burial of benthic organisms through their effect on bed erosion/accretion and bedform migration.

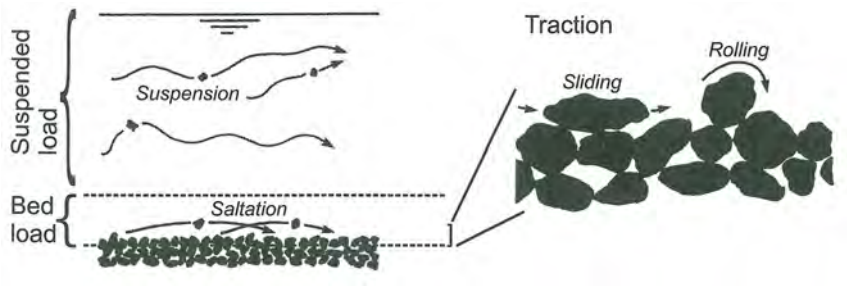

Figure 2.5: *Schematic representation of sediment transport modes showing idealised grains paths (From Masselink and Hughes, 2003 and modified after Allen, 1994).*

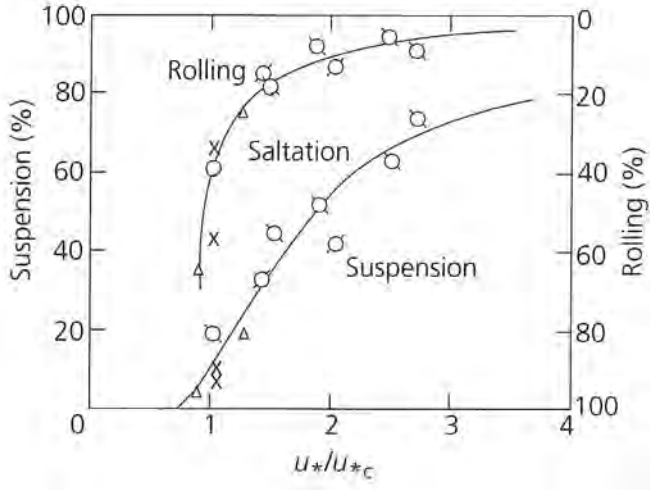

Figure 2.6: *Laboratory data from Francis (1973) showing modes of sediment transport as a function of the dimensionless shear velocity* u_*/u_{*c} *(From Allen, 1997).*

2.4.3 Bedform migration and other changes in bed elevations

Bedforms are periodically recurring irregularities in bed elevation, or more or less regularly-spaced waves in the surface of the seabed (Allen, 1985; Allen, 1997). A variety of bedform types occur on the continental shelf and can be distinguished by their morphology and dimensions. A summary of the morphology and some examples are shown in Figures 2.7 and 2.8 and dimensions are listed in Table 2.1.

Table 2.1: List of bedforms found on the continental shelf and their dimensions (Allen, 1997).

BEDFORM	HEIGHT	SPACING (OR WAVELENGTH)
Wave ripples	<0.2 m	0.02-1.0 m
Small current ripples	<0.06 m	0.1-0.2 m
Dunes (or sand waves)	0.06-1.5 m	0.6-100 m
Sand banks	O(10) m	O(100s-1000s) m

In order to progress through a sequence of covering – uncovering – and recovering a benthic community the bedform has to migrate a full wave length. At the broadest level bedforms can be separated according to wave-length-scale into, from smallest to largest, ripples, dunes, and banks. For quasi-steady flow conditions the time-scale for migration of ripples is of the order minutes to hours and for dunes it can be hours to weeks or more. For sand banks it is of the order months to years. The episodic development and migration of ripple fields on the seabed during temperate storms or tropical cyclones may result in patch creation and lead to an ecological disturbance regime, if the storm frequency is appropriate for the community's succession time-scale. Alternatively, the migration time-scale itself of dunes and banks (months to years) may be directly appropriate for creating an ecological disturbance regime. Whether bedform migration is sufficient to cause a disturbance will obviously depend on the scale of the bedform relative to the scale of the species present. For example, ripple migration is not likely to disturb a patch of seagrass, in fact ripples are commonly observed in healthy seagrass beds. Sand bank migration on the other hand has been hypothesised to be responsible for die-back of seagrass beds in Torres Strait, for example (Daniell et al., 2008).

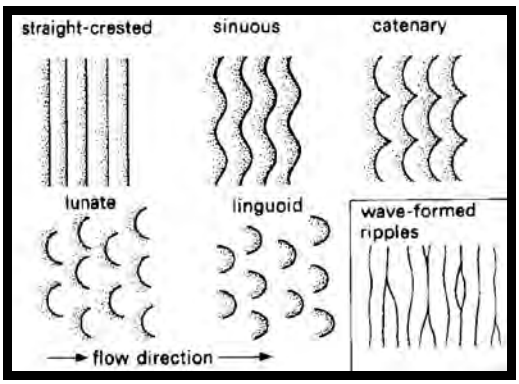

Figure 2.7: *Schematic diagram showing plan view of crest lines for 2-dimensional and 3-dimensional bedforms (From Tucker, 1995).*

The key to determining a surrogate for ecological disturbance due to bedform migration is to be able to identify the existence of a bedform type, in particular those with a scale larger than the benthic species present, and the time-scale that it migrates. Bedform phase diagrams can be useful in this regard, although they only apply to the smaller scale bedforms, i.e. ripples and dunes (Figure 2.9). They show ranges of environmental parameters for which different bedform types exist and are in approximate equilibrium with the flow regime. Implicit in the statement of approximate equilibrium is that they are migrating, because they must be moving in order to respond and equilibrate with the flow conditions. Bed shear stress and grain diameter are the primary environmental variables

controlling the equilibrium bedforms present. In general, bedform scale increases (from ripples to dunes) with both bed shear stress and grain size.

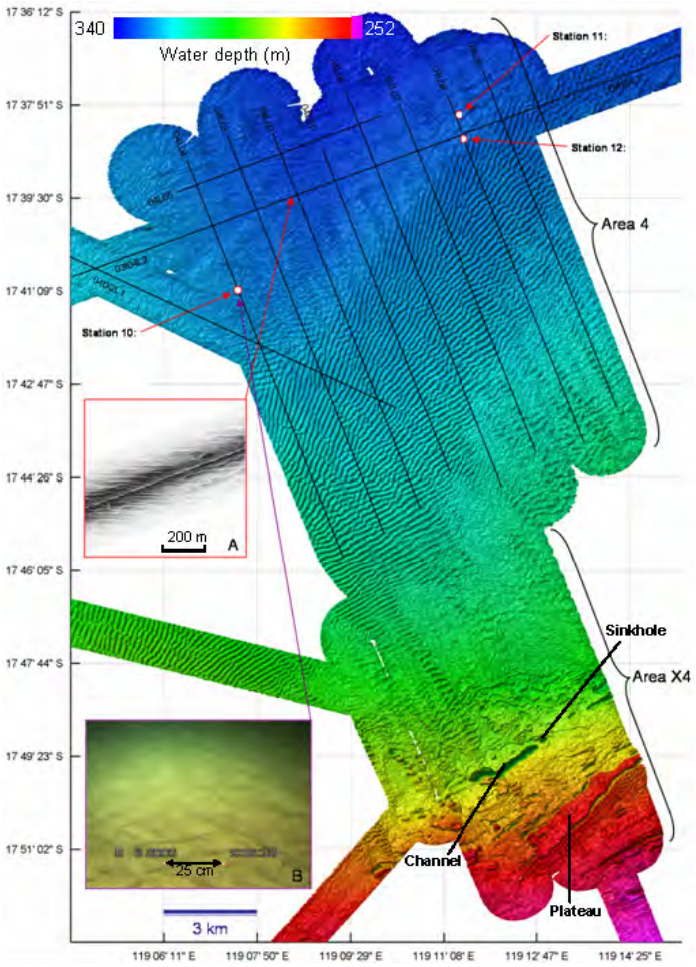

Figure 2.8: *Hill-shaded colour image of multibeam bathymetry showing an extensive dune field in approximately 300 m water depth on the northwest shelf of Australia. Inset is a photograph of small current ripples that occur superimposed on the larger dunes (From Jones et al., 2007).*

The dynamics of all bedforms are controlled by spatial gradients in the sediment transport rate over a length scale commensurate with their wave length. Where the transport gradient is decreasing more sediment is coming in than exiting and the seabed will locally accrete, and where the gradient is increasing more is exiting than coming in and it will locally erode. In the case of ripples and dunes there gradients periodically reverse over a distance of centimetres to hundreds of metres. This is a distance over which sediment availability is often uniform. In contrast, banks are associated with transport gradients that occur over kilometres, a distance over which sediment availability is commonly highly variable. Furthermore, the larger scale banks are rarely if ever in equilibrium with the instantaneous or short-term flow regime. They reflect the aggregate flow regime over long time-scales. In short, they are controlled by large-scale factors such as sediment availability and flow

regime, which makes their dynamics characteristically site specific. As a consequence, their existence and migration are difficult to predict, and cannot be generalised in the form of a bedform phase diagram (cf. Figure 2.9).

2.5 DISTURBANCE REGIMES AND THE AUSTRALIAN SHELF

To create a disturbance, the flow-induced bed shear stress must clear a patch of habitat through direct damage to the benthos or through abrasion, light reduction, burial or displacement by sediment transport and/or bedform migration. A current type, or combination of current types, that causes periodic or episodic disturbances meeting the IDH criteria will give rise to a disturbance regime (i.e. it will create patches of disturbed habitat that coexist with patches of partly recovered habitat and other patches of fully recovered habitat; Figure 2.1).

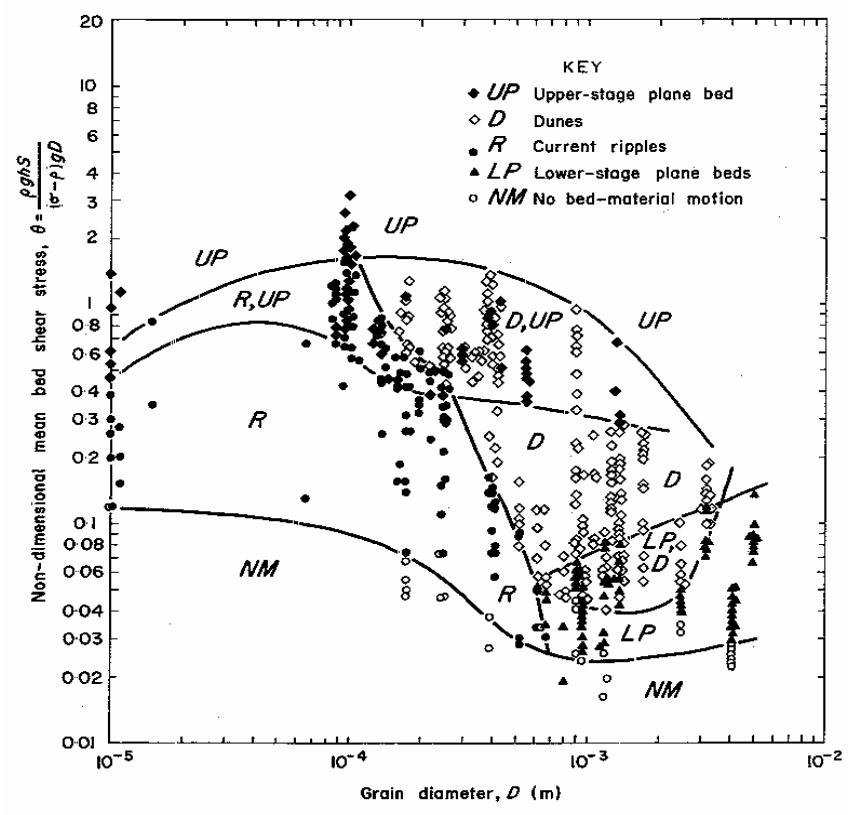

Figure 2.9: *Bedform phase diagram plotted on the non-dimensional bed shear stress (Shield's parameter) – grain diameter plane. A total of 595 observations are represented, but many have been excluded (except critical or limiting ones) for clarity (from Allen, 1984).*

Tidal currents are an example of periodic flows. Plants and animals that live in tidal environments are affected by the fortnightly neap-spring cycle of the tides and are exposed to intense spring tidal currents in macrotidal environments. Tidal environments may be extremely energetic and cause intense suspended and bedload transport. However, tidal currents do not constitute an intermediate

disturbance regime in the context of benthic ecology, because the recurrence interval of tides is short compared to life-cycles and recruitment of benthic communities (Figure 2.3 and 2.10). Also, since tidal currents would not be expected to create a patch of newly disturbed habitat over daily or fortnightly intervals, there are no patches of disturbed habitat present in such a high-frequency current regime. The benthos existing in a tidal environment will have adapted to the energetic reversing currents that occur twice-daily (or daily in diurnal tidal systems) and they have evolved to feed and reproduce in such an environment, with different communities occurring along the gradient of tidal bed shear stress (Warwick and Uncles, 1980; Long et al., 1997).

At the opposite end of the temporal spectrum are disturbances that occur so infrequently that the processes of colonisation and re-establishment of undisturbed seafloor are only rarely present together (Figure 2.10). For the vast majority of the time there are no patches of disturbed habitat present. Examples of such current-related disturbances are shelves subject to tsunami or mass failures that occur only over millennial or geological timescales (Figure 2.10).

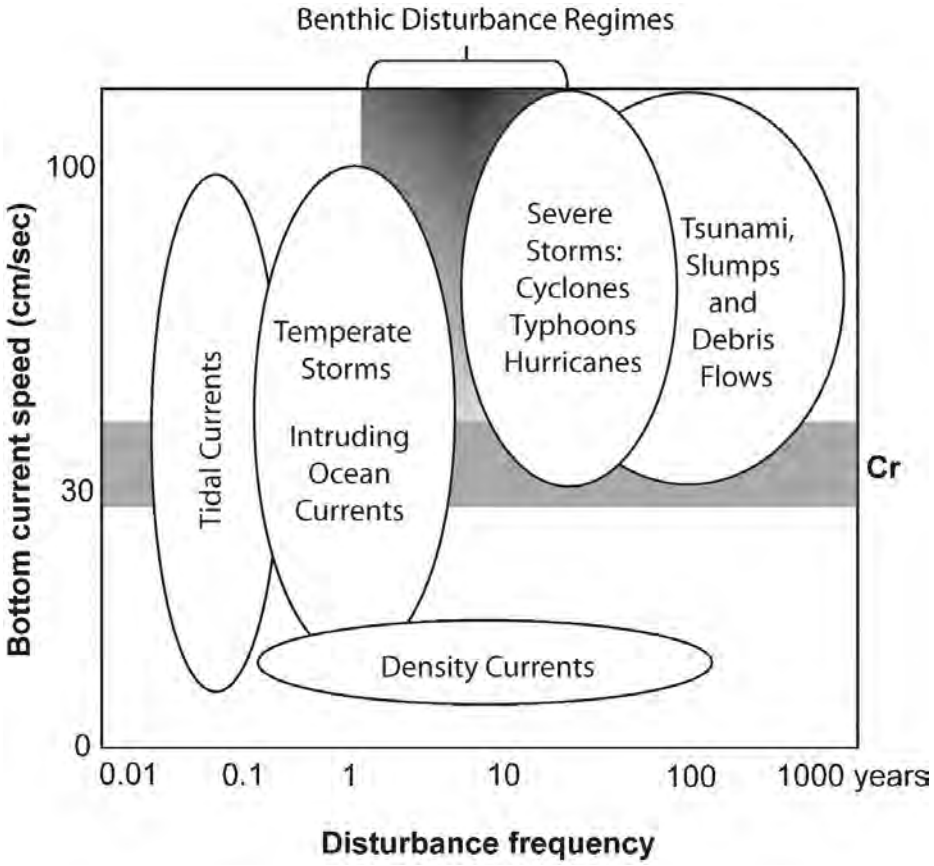

Figure 2.10: *Conceptual diagram showing the typical frequency and magnitude of shelf-current types in relation to those capable of causing a benthic disturbance regime at a typical, mid-shelf geomorphic setting (from Harris, 2010). See text for further explanation.*

In the case of a true disturbance regime, the physical process must be infrequent enough that the community is adapted to the lower energy conditions that occur between current events. For this reason, the gradation between true disturbance regimes and frequent, high-energy storm or intruding ocean current events is best viewed as a continuum rather than a distinct boundary (Figure 2.10). In a similar way, the intensity of the bed stress that causes a disturbance (the vertical axis in Figure 2.10) is also a continuum rather than a distinct boundary, because different organisms will be affected by high bed stress events in different ways. Marine biologists are well aware that benthic plants and animals have physical attributes that have evolved to yield some advantage for particular physical environments (see review by Mann and Lazier, 2006). For some fragile, epibenthic plants or animals such as bryozoans, exceedance of the critical threshold value by any amount will be catastrophic, resulting in dislodgement, breakage and fragmentation. Other species such as heavily calcified forms, deposit feeders and infauna, are able to withstand more intense bed stress events and can recover quickly after the event is over (Hall, 1994).

The process must be great enough in both magnitude and spatial extent to create a patch of habitat that is disturbed enough to create space for opportunistic species to colonise. For example, density currents formed on the continental shelf by processes that cool shelf waters and/or increase its salinity are known to occur at different frequencies (e.g. Williams and Bindoff, 2003; Nunes Vaz et al., 1990). Where measurements have been made it has been shown that such density flows on the shelf are mostly very weak (~10 cm/sec), and are thus incapable of causing a physical disturbance of their own accord (although cascades of dense shelf water may attain much greater speeds where they descend submarine canyons, these are located on the continental slope rather than on the shelf; e.g. Canals et al., 2004). Therefore, although density currents may occur at intervals comparable to the life-cycles and recruitment of benthic species, they are unlikely to cause a physical disturbance because of their low intensity.

Processes that occur within the frequency range and with a great enough intensity to cause a disturbance (i.e. the upper-centre of Figure 2.10) are temperate storms, the intrusion of ocean currents onto the continental shelf and severe storms. The frequency of occurrence of these high-energy events coincides with the time required by opportunistic colonisers to move in and for the patch to recover to a pre-disturbed state, resulting in patches of disturbed and undisturbed habitat to coexist.

Figure 2.11 presents a regionalisation of the Australian shelf according to the principal drivers for sediment transport. A mixture of tidal currents and tropical cyclones dominate the northern half of the Australian shelf, whereas temperate storms and swell are important across the southern half.

Historical tropical cyclone tracks across the Australian shelf are largely constrained between 10°S and 25°S. The cyclone season extends from December to April with average occurrences of 1.5 and 2.5 cyclones per year for the northeast and northwest margins, respectively (Lourensz, 1981). Temperate storms tracking east-west across the southern margin in winter are responsible for episodic large wave events; annual return significant wave height up to 8.7 m, superimposed on persistent high energy swell with a modal significant wave height of 2-3 m (Hemer, et al., 2009). Intruding ocean currents onto the shelf are of minor, localised importance in the vicinity of Fraser Island (Queensland) and Exmouth (Western Australia).

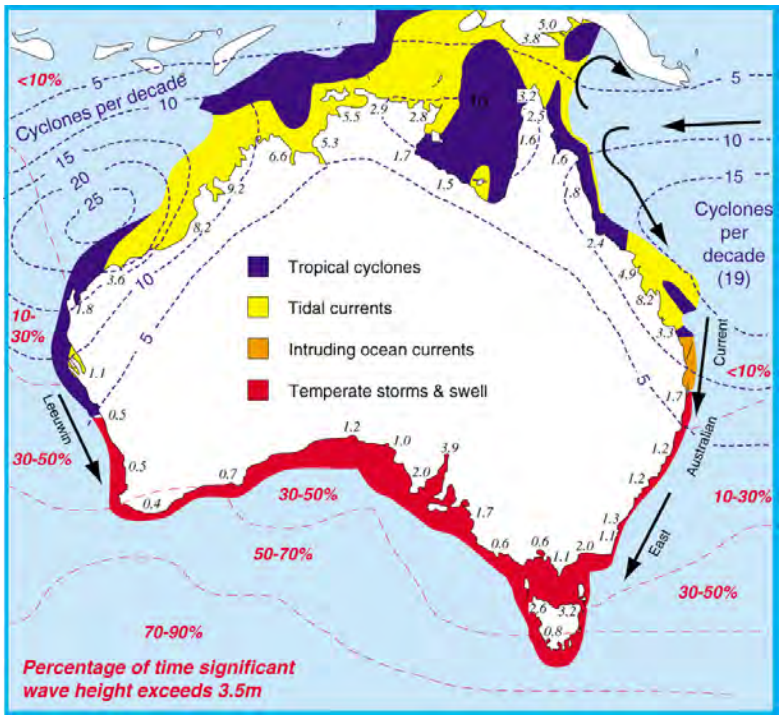

Figure 2.11: *Division of the Australian shelf (after Harris, 1995) into regions in which sediment transport is caused mainly by tidal currents, currents derived from tropical cyclones, ocean swell and storm-generated currents, and intruding ocean currents. Contours of tropical cyclone frequency per decade are from Lourensz (1981) and contours forsignificant wave height percentage exceedence are from McMillan (1982). Mean spring tide ranges indicated along the the coastline are derived from the Australian National Tide Tables. The location and direction of flow of major ocean currents are indicated.*

Temperate and severe (tropical cyclone) storms control sediment transport over 82% of the shelf area, whereas tidal currents and intruding ocean currents are predominant over 17.4% and 0.6% of the shelf area, respectively (Porter-Smith et al., 2004). In the context of the IDH, up to 82.6% of the Australian shelf could potentially exist under a disturbance regime that assists in maximising biodiversity.

3. Methods – GEOMACS model

3.1 INTRODUCTION

GEOMACS is Geoscience Australia's GEological and Oceanographic Model of Australia's Continental Shelf. The precursor to GEOMACS was GEOMAT (GEological and Oceanographic Model for Australia's ocean Territory), which was fully described by Harris et al. (2000). GEOMAT modelled the role of waves and tides acting independently on the seabed. GEOMACS represents a considerable refinement by modelling the combined effect of waves, tides and ocean circulation. The GEOMACS model has also been described previously by Hemer (2006).

3.2 MODEL OVERVIEW

GEOMACS aims to hindcast the bed shear stress in water depths representative of the continental shelf. The inputs are hindcast waves, tides and ocean circulation from component models, as well as bathymetry and sediment texture (grain size). The output is an hourly time series of total combined bed shear stress on a 0.1° grid covering Australia's continental shelf. The shelf is pragmatically defined as water depths <300 m. The hindcast time period is 1 March 1997 to 28 February 2008 (11 years).

3.2.1 Input A - waves

The hindcast wave conditions were obtained using the WAM model – a third generation ocean wave prediction model (Hasselmann et al., 1988). Implementation of the WAM model for the Australian region (AusWAM) was performed by the Australian Bureau of Meteorology (BOM) using their high resolution atmospheric model on a 0.1° grid covering 110–156° longitude and 7–46° latitude (e.g. Greenslade, 2001). The hindcast wave conditions from the model were significant wave height H_s, mean wave period T_m and wave direction θ as 6-hourly time series for the 11-year GEOMACS model period. The time series were subsequently interpolated to hourly values to match the temporal resolution required to represent tidal currents.

The WAM model integrates the basic transport equation describing the evolution of a two-dimensional ocean wave spectrum without any assumptions concerning the evolving spectral shape. Energy dissipation due to whitecapping is included in the model, and energy dissipation due to bottom friction as well as refraction is included in the finite-depth version of the model (Hasselmann et al., 1988). Depth-induced wave breaking, however, is not included. For this reason and the limited grid resolution compared to increased bathymetric complexity in shallow water, the AusWAM hindcasts are considered to be of limited value for water depths <20 m (see also Booij et al., 1999).

First-order linear wave theory was used to compute the peak wave orbital velocity U_w from the hindcast H_s and T_m, i.e.

$$U_w = \frac{\pi H_s}{T_m \sinh(kh)} \tag{3.1}$$

where the wave number $k = 2\pi/L$, L is the wave length and h is the water depth. Since the wavelength is not hindcast, the wave dispersion equation relating L and T was used to evaluate k or more precisely kh. The general form of the dispersion equation for linear waves is implicit, but there are several approximations for kh available in the literature. For example, the following is accurate to 0.1%

$$(kh)^2 = y^2 + y\begin{pmatrix} 1 + 0.666y + 0.355y^2 + 0.161y^3 \ldots \\ + 0.0632y^4 + 0.0218y^5 + 0.00654y^6 \end{pmatrix}^{-1} \tag{3.2}$$

(Hunt, 1979) where $y = \omega^2 h/g$ and the wave radial frequency $\omega = 2\pi/T$.

3.2.2 Input B - tides

The tidal current vector was predicted using an application of the linearised shallow water equations that included parameterised corrections for dissipation, tidal loading and ocean-shelf attraction (Egbert et al., 1994). The regional implementation of this tidal model was fed tidal elevations along open boundaries by the global ocean tide model described by Andersen et al. (1995). The implementation on the Australian shelf is described at length by Harris et al. (2000) and Porter-Smith et al. (2004) and only the salient points are reiterated here.

The tide model was initially implemented on a 0.067° grid covering 109–160° longitude and 0–45° latitude. The solution was obtained using time-stepping on an Arakawa C grid by applying periodic forcing from homogeneous initial conditions. Dissipation was approximated using the quadratic expression for the bottom drag coefficient K in terms of water depth h;

$$K = \frac{K_o}{(\max(h, h_o))^2} \tag{3.3}$$

where K_o is the bottom drag coefficient at depth h_o. A choice of $K_o = 0.05$ and the minimum depth of $h_o = 20$ was made after extensive testing, because it worked well for most regions (Porter-Smith et al., 2004). The model was improved through data assimilation techniques using both satellite altimetery data and coastal tide gauge data.

Ocean tide elevations were derived from the NASA ocean altimeter Pathfinder products for the TOPEX/POSEIDON satellite. The Australian National Tidal Facility provided a set of harmonic constituents for 57 standard ports around Australia. Constituents from 16 of these ports were used to supplement altimeter data and produce constituent sets at a total of 195 locations across the GEOMACS domain, which were blended into the tide model. Harmonics from the remaining ports were used to tune and validate the tide model. The blending approach was based on Kantha (1995); the predicted tidal height H_t at the 195 locations was substituted by a weighted mean of the predicted tidal height by the model H_{pred} and the observed height H_{obs} using

$$H_t = wH_{obs} + (1-w)H_{pred} \tag{3.4}$$

where the prediction weight w was determined for each constituent individually. The modified height H_t was subsequently used to calculate the sine and cosine coefficients of the east and north components of the tidal current velocity. These were interpolated onto the GEOMACS 0.1° grid and hourly velocity components were calculated for the hindcast time period using

$$u = \sum_{i=1}^{4} \frac{u_{i\cos}\cos(\omega_i t) + u_{i\sin}\sin(\omega_i t)}{h} \quad \text{and} \quad v = \sum_{i=1}^{4} \frac{v_{i\cos}\cos(\omega i t) + v_{i\sin}\sin(\omega_i t)}{h} \tag{3.5}$$

where u and v are the east and north components of the tidal current velicoty; u_{icos}, v_{icos}, u_{isin} and v_{isin} are the cosines and sines of the u and v components of the mass flux for the i^{th} consitiuent; and ω_i is the angular frequency of the i^{th} constituent. For the subsequent calculation of bed shear stress the modelled tidal current velocity was assumed to represent that at 1 m above the bed.

3.2.3 Input C – ocean currents

A climatic representation of wind- and density-driven ocean currents was included in the GEOMACS model based on four years of output from the Ocean Circulation and Climate Advanced Modelling (OCCAM) project. The OCCAM model is a primitive equation numerical model of the global ocean based on the Bryan-Cox-Semtner ocean model, but including a free surface and improved advection schemes (Webb et al., 2000). In the region of interest here, a regular 0.25° grid was employed with 36 variably spaced layers in the vertical extending from 20 m to 5500 m depth. The wind stress used to force the OCCAM model was the monthly-averaged European Centre for Medium-range Weather Forecasting (ECMWF) wind stress climatology calculated by Siefridt and Barnier (1993). The surface fluxes of heat and freshwater necessary to match the Levitus global average data set (Levitus, 1982) were implemented to drive baroclinic motions. Full details of the OCCAM model are given by Webb et al. (2000).

Unfortunately the freely-available OCCAM model output did not coincide with the GEOMACS hindcast period. Consequently, wind-driven wave events are not coupled in time with wind-driven current events. Furthermore, the wind-driven current is forced by monthly-averaged wind fields and

therefore does not represent synoptic events. The purpose of including the OCCAM model results in GEOMACS is to represent the seasonal contribution of wind- and density-driven currents to shelf sediment transport. The four years of OCCAM model output used here (years 8-11) was obtained gratis from the OCCAM project, and included east and north components of ocean current velocity every 15 days on the 3D grid. For the subsequent calculation of bed shear stress the velocity in the model layer locally closest to the seabed was assumed to represent that at 1 m above the seabed. The OCCAM model output was interpolated to the GEOMACS 0.1° grid and hourly time-step and was applied recursively over the 11 year hindcast period. The OCCAM-predicted current velocity was linearly vector added to the predicted tidal velocity to obtain an hourly estimate of total current velocity (Hemer, 2006).

3.2.4 Bathymetry and sediments

Water depth is required to calculate the wave orbital velocity from the input wave conditions (Equation 3.1), and to frictionally dampen the tide (Equation 3.2) prior to calculating the tidal current velocity (Equation 3.5). Geoscience Australia's 250 m resolution bathymetry model was used and re-interpolated to the GEOMACS 0.1° model grid.

Sediment grain diameter is required to estimate the hydraulic roughness of the seabed prior to calculating the bed shear stress (Section 3.2.2). Geoscience Australia's marine sediments database (MARS) provided the necessary grain size information. All available samples in the data base containing quantitative grain size information were used and the mean grain size was computed for each sample location. The mean grain sizes were interpolated on to the GEOMACS 0.1° model grid using an inverse distance-weighting scheme. In areas where little to no data was available a constant grain size equal to medium-coarse sand (0.9 mm) was used. The model output combined-flow bed shear stress was found to be relatively insensitive to changes in mean grain size. A doubling of the grain size increased the bed shear stress by approximately 15% (Hemer, 2006).

3.2.5 Model algorithm and output

Employing the wave-induced oscillatory current, combined tidal and wind-driven current, and grain size described in Section 3.2.1, the bed shear stress vector was calculated using the one-dimensional bottom boundary layer model SEDTRANS (Li and Amos, 2001). SEDTRANS is based on the non-linear, combined wave-current boundary layer model developed by Grant and Madsen (1986), but also incorporates additional hydraulic roughness due to the presence of bedforms. Determination of the bed shear stress due to combined currents and waves τ_{cw}

$$\tau_{cw} = \rho u_{*cw}^2 \tag{3.6}$$

where ρ is the water density and u_{*cw} is the shear velocity due to combined currents and waves, is a three-step process (see Li and Amos, 2001). Noting that the subscripts *w*, *c* and *cw* refer to waves alone, currents alone and combined currents and waves throughout, the first step requires the estimation of a combined current and wave friction factor f_{cw} by solving

$$\frac{1}{4\sqrt{f_{cw}}} + \log\left(\frac{1}{4\sqrt{f_{cw}}}\right) = \log\left(\frac{C_r u_b}{\omega z_o}\right) + 0.14\left(4\sqrt{f_{cw}}\right) - 1.65 \tag{3.7}$$

through iteration, where u_b is the nearbed maximum wave orbital velocity, ω is the wave angular frequency, $z_o = k_b/30$ is the hydraulic bed roughness and C_r is the first assumed relative strength ratio of waves to currents. Different values of roughness height k_b have to be used to compute the various components of bed shear stress. In the second step the maximum wave shear velocity u_{*w} is calculated using the initial estimate of C_r and f_{cw} from Equation 3.7 and substituting into

$$u_{*w} = \sqrt{\frac{C_r f_{cw} u_b^2}{2}} \tag{3.8}$$

and the shear velocity due to combined currents and waves is then obtained from

$$u_{*cw} = u_{*w}\sqrt{C_r} \tag{3.9}$$

The near-bed velocity profiles are

$$u_z = \frac{u_{*c}^2}{\kappa u_{u*cw}} \ln\left(\frac{z}{z_o}\right), \quad z \le \delta_{cw} \tag{3.10}$$

and

$$u_z = \frac{u_{*c}}{\kappa} \ln\left(\frac{z}{z_{oc}}\right), \quad z \ge \delta_{cw} \tag{3.11}$$

where u_{*c} is the current shear velocity and z_{oc} is the apparent bed roughness experienced by the current in the presence of waves, and $\delta_{cw} = 2\kappa u_{*cw}/\nu$ is the thickness of the current-wave boundary layer. By matching the current of the outer layer (Equation 3.11) and that of the wave boundary layer (Equation 3.10) at the height of δ_{cw}, the current shear velocity can be computed from

$$u_z = \frac{u_{*c}}{\kappa}\left[\frac{u_{*c}}{u_{u*cw}} \ln\left(\frac{\delta_{cw}}{z_o}\right) + \ln\left(\frac{z}{\delta_{cw}}\right)\right] \tag{3.12}$$

where u_z is the input mean flow velocity at the height *z* (in this case 1 m) above the bed. The third step uses the results from step 2 to compute a revised value of C_r from

$$C_r = \sqrt{1 + 2\left(\frac{u_{*c}}{u_{*w}}\right)^2 \cos\phi_b + \left(\frac{u_{*c}}{u_{*w}}\right)^4} \tag{3.13}$$

where ϕ_b is the angle between the wave and current inside the boundary layer. This revised C_r is then used to repeat the steps until a convergence of C_r is achieved and the associated u_{*cw} is determined, which is then used to calculate τ_{cw} from Equation 3.6.

3.3 SUMMARY

The GEOMACS model has the following inputs: (1) near-bed oscillatory currents due to wind waves and swell; (2) near-bed currents due to tides; (3) near-bed currents due to wind- and density-driven circulation; (4) bathymetry and (5) grain size. The first three are provided by hydrodynamic models; the WAM ocean wave model (Hasselmann et al. 1988), a linearised tidal model (Egbert et al., 1994), and the OCCAM ocean circulation model (Webb et al., 2000), respectively. The two remaining inputs are from a bathymetric grid and sediment data base developed and maintained by Geoscience Australia (Whiteway, 2009; Passlow et al., 2005). GEOMACS uses these inputs together with a one-dimensional wave boundary layer model (Grant and Madsen, 1986; Li and Amos, 2001) to calculate the total bed shear stress due to combined currents and waves. GEOMACS output is hourly time series of bed shear stress covering an 11-year period (1 March 1997 to 28 February 2008) on a 0.1° grid covering Australia's continental shelf (water depths <300 m). This GEOMACS data set is used here to derive potential surrogates for marine biodiversity.

4. Results – Parameters representing seabed exposure

4.1 INTRODUCTION

Seabed exposure refers to the general magnitude of bed shear stress that the benthos is exposed to. It can, therefore, be represented by statistical parameters that describe the bulk of the frequency distribution of bed shear stress occurring at a given location. For example, measures of central tendency (mean mode, median) and spread (e.g. quartiles, interquartile range and standard deviation) of the distribution. No consideration of the nature of the benthic community is made (see Sections 2.1 and 2.2).

4.2 NATIONAL OVERVIEW

Figure 4.1 shows an example time series and the corresponding frequency distribution of the temporal bed shear stress at an arbitrary location on the shelf. The time series is strongly tidal and punctuated by episodic cyclone events (Figure 4.1a and b). The distribution is right-skewed; with the mode and median less than the mean, which is strongly influenced by a relatively few extreme values (Figure 4.1c). This is characteristic of most locations on the shelf, due to either the presence of infrequent, large magnitude events and/or the fact that the bed shear stress varies with the velocity squared (see Equation 3.6).

Several parameters describing the distribution of temporal bed shear stresses at each location on the GEOMACS grid have been calculated and are listed in Table 4.1. Items 1 and 3-8 are self evident. The trimmed mean is the mean of the values excluding the upper and lower 25% of the distribution. The mean daily standard deviation was calculated by first calculating the standard deviation of values in each day and then finding the mean of those daily standard deviations. The parameter is meant to represent the seabed exposure to tidal currents. The percentage of time the bed shear stress is greater than 0.4 Pa was included, because previous studies have suggested benthic communities exposed to such stresses tend to have higher biodiversity (Haywood et al., 2007). An analogue of work rate at exceeding 0.4 Pa is denoted here as R and is calculated using

$$R = \frac{\int_0^{t_{\max}} \tau_{>0.4}.dt}{\int_0^{t_{\max}} \tau.dt} \qquad (4.1)$$

where t is time, t_{max} is the length of the time series, τ is the bed shear stress, and $\tau_{>0.4}$ is that part of the bed shear stress time series where values exceed 0.4 Pa.

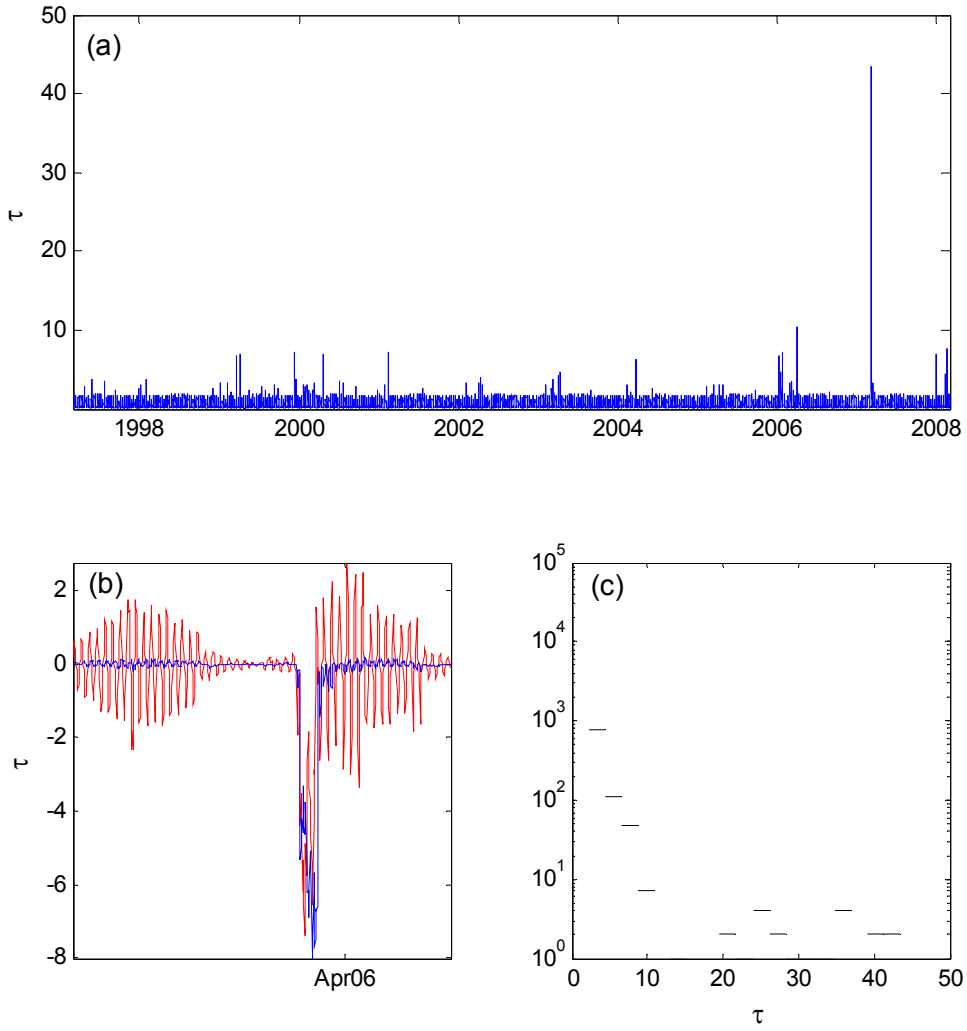

Figure 4.1: *Example of the combined bed shear stress (Pa) output from the GEOMACS model for a location on the Pilbara shelf (19.5°S, 119.5E°): (a) magnitude time series, (b) east (red) and north (blue) components of bed shear stress for a one month period, and (c)frequency histogram of shear stress magnitude.*

The range in magnitude of each parameter listed in Table 4.1 is large at the national scale. Frequency distributions of the spatial variability in each are shown in Figure 4.3, and they are also characteristically right-skewed. This is largely due to typical shelf hypsometry in which shallower depths occupy a relatively smaller shelf area, but are generally associated with the largest bed shear stresses. In order to highlight variability in the data, maps showing spatial variation in the parameters calculated to represent seabed exposure have been log-transformed (Appendix A).

Table 4.1: List of parameters used to describe the temporal distribution of bed shear stresses on the Australian shelf, and thereby represent seabed exposure.

ITEM NO.	PARAMETER	ITEM NO.	PARAMETER
1	Mean	7	Interquartile range
2	Trimmed mean	8	Standard deviation
3	Median (50^{th} percentile)	9	Mean daily standard deviation
4	Mode	10	% time >0.4 Pascals
5	25^{th} percentile	11	*R* (Eq. 4.1)
6	75^{th} percentile		

Spatial patterns in the mean, trimmed mean, median, 25^{th} and 75^{th} quartiles of bed shear stress are consistent, with highest values on the northern half of Australia's shelf occurring on the tide-dominated Pilbara and Kimberley shelves, Torres Strait and southern Great Barrier reef (Figures A.1-A.3 and A.5-A.7). On the southern half of Australia's shelf there is high seabed exposure due to accelerated tidal streams in Bass Strait, but principally the most exposed areas are constrained to the coastal strip exposed to the prevailing swell direction (see Section 4.3). The pattern for the modal bed shear stress looks different (Figure A.4), because in tide-dominated areas the modal bed shear stresses are small as the tide reverses through zero velocity, typically twice each day. Interestingly, in the case of parameters 8-11 (Table 4.1) the spatial variability is more complex (Figures A.8-A.11). This complexity and its possible implications for biodiversity are discussed further in Section 6.

4.3 REGIONAL EXAMPLES

To assist with interpretation of the national scale maps presented in Appendix A, three regions have been selected to exemplify wave- tide- and cyclone-dominated shelves (Figure 4.3). Furthermore, specific sites have been identified to exemplify the inner and outer shelf in each region. The inner shelf site was selected from approximately 40 m water depth and the outer shelf from approximately 150 m water depth in each region (Figure 4.3). The shelf extent that each of these examples represents can be determined by comparing with Figure 2.10.

On a wave-dominated shelf the seabed exposure (represented by the mean bed shear stress in Figure 4.4a) is determined by a combination of exposure to the prevailing wave direction, water depth and wave period. In the example from the southern margin (Figure 4.2), the prevailing wave direction is from south-southwest. The seabed areas with greatest exposure are clearly closest to the coast where the shallowest water depths occur in the region. The water depth at which no wave-induced motion at the seabed occurs is related to the wavelength and, through the wave dispersion relation, the wave period. So the distance offshore that the coastal zone of relatively high seabed exposure will extend on wave dominated shelves will depend on the steepness of the shelf and the predominant wave

period. Both relatively steep shelves and relatively short-period waves will result in the narrowest coastal zone of high seabed exposure, whereas both low-gradient shelves and long-period waves will result in the broadest zone. At a regional scale on wave-dominated shelves the incident wave conditions are spatially constant. The pattern of seabed exposure will therefore largely parallel bathymetry, with additional shadow zones of low exposure in the lee of prominent coastal topography such as major headlands and islands. Compare, for example, the seabed exposure in Figure 4.4a associated with the coastal protuberances to that in the embayment between.

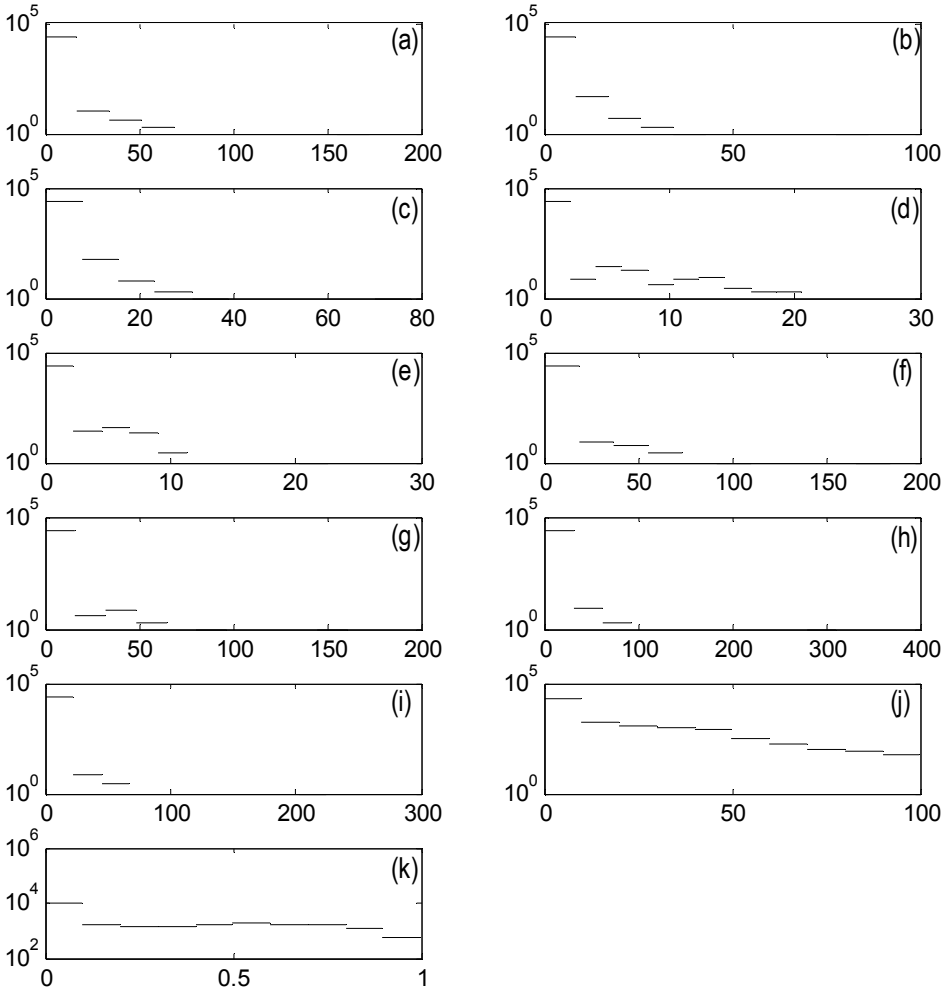

Figure 4.2: *Histograms (presented as number of grid cells) of: (a) mean bed shear stress; (b) trimmed mean bed shear stress; (c) median bed shear stress; (d) modal bed shear stress; (e) 25th quartile bed shear stress; (f) 75th quartile bed shear stress; (g) interquartile range of bed shear stress; (h) standard deviation of bed shear stress; (i) mean daily standard deviation of bed shear stress; (j) percentage-time bed shear stress exceeds 0.4 Pa; and (k) R (Eq. 4.1).*

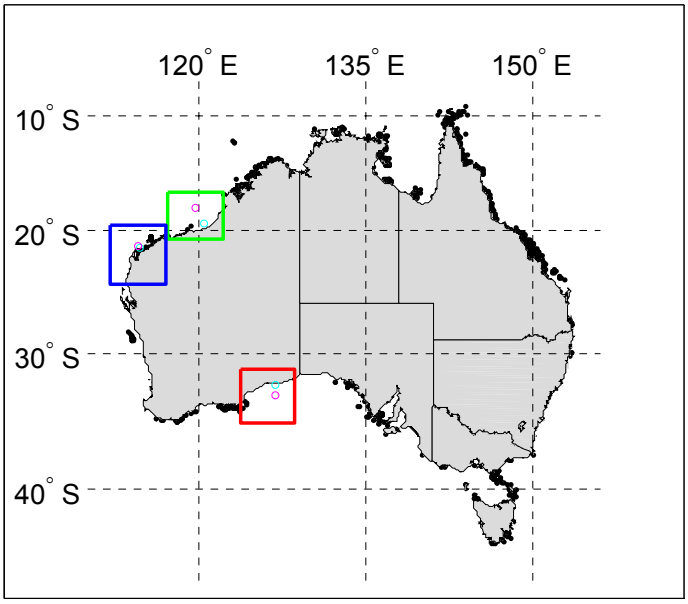

Figure 4.3: *Map showing locations and extents of regions used to represent wave (red), tide (green)and cyclone(blue) dominated shelves. The cyan and magenta open circles show locations from where example time series are presented (Figures 4.5 to 4.7) to represent the inner shelf (40 m water depth) and outer shelf (150 m water depth), respectively.*

There is a clear distinction in the magnitude and the frequency content of the bed shear stress between the inner and outer shelf in a wave-dominated region. The normalised bed shear stress time series from the inner shelf site in the southern margin region shows a variable time series punctuated by episodic, large-magnitude events (Figure 4.5a). The bed shear stress can reach 200-500 times the median value during these episodic events. In contrast, the time series from the outer shelf shows a much clearer annual and spring-neap signal in the time series, and episodic events reaching only 10-20 times the median bed shear stress (Figure 4.5b). At both the inner and outer shelf sites the spectral energy in the bed shear stress signals is greatest at inter-annual frequencies (Figure 4.5c). At intra-annual frequencies, however, the frequency content in the signals differs greatly between the two. On the inner shelf the spectral energy remains high at seasonal frequencies and then rolls off rapidly through the higher (tidal) frequency band. In contrast, at the outer shelf site, seasonal frequencies are relatively less important and the tidal frequency band is relatively more energetic. To summarise, on a wave-dominated shelf (a) seabed exposure increases shoreward in the cross-shelf direction; (b) inter-annual cycles in exposure are important across the full shelf width; (b) seasonal cycles (where they exist) are only apparent on the inner shelf (specifically, inside wave base); (c) other processes such as tides are more important than waves at intra-annual frequencies on the outer shelf (specifically, outside wave base).

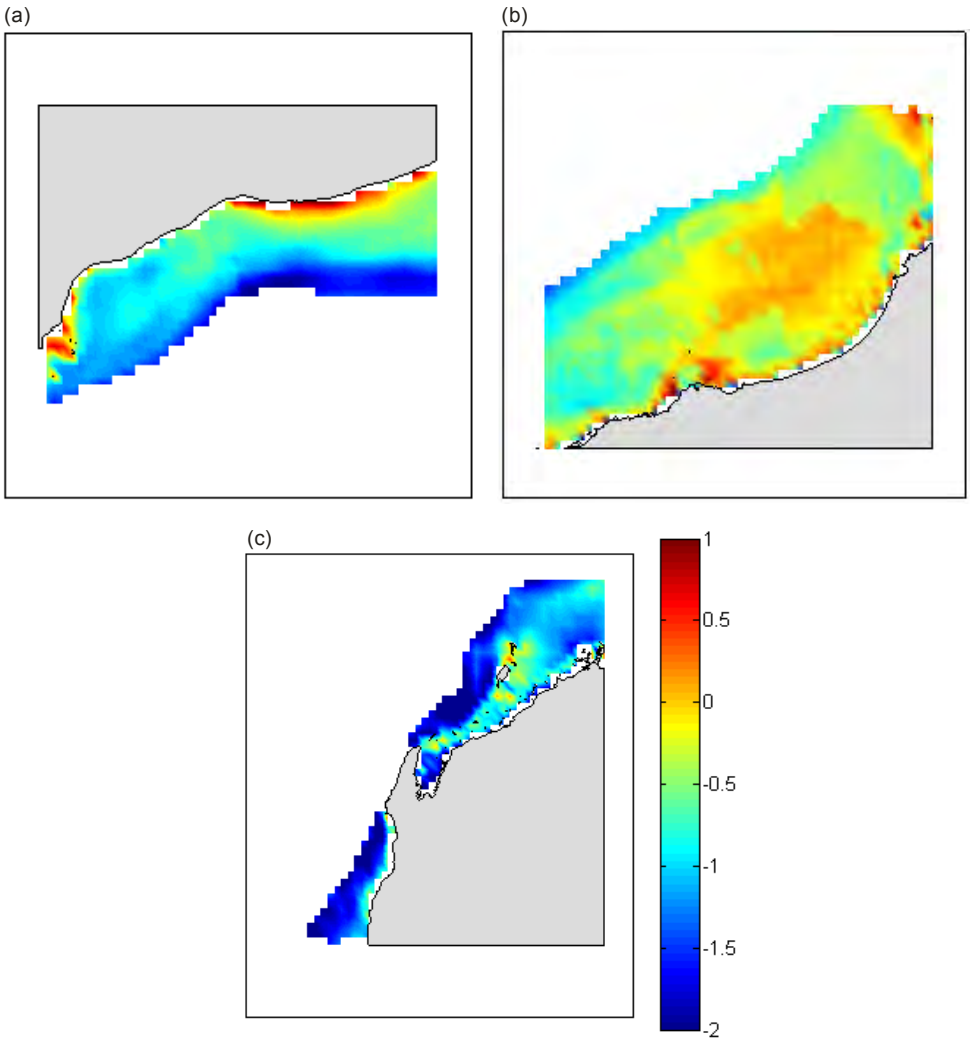

Figure 4.4: *Logarithm of the mean bed shear stress due to combined waves, tides and currents. The examples shown are for a (a) wave-dominated shelf, (b) tide-dominated shelf, and (c) cyclone-influenced shelf. The location of each region is shown on Figure 4.3.*

The pattern of seabed exposure is markedly different on a tide-dominated shelf. The tide mobilises the entire water column at all shelf depths so there is no equivalent to a wave base. The seabed exposure on tide-dominated shelves can be relatively high even on the outer shelf, particularly if meso- to macro-tide ranges are involved (Figure 4.4b; see also Harris, 1994). Seabed exposure can also be high in locations where tidal streams are constrained to channels between offshore reefs, islands and the mainland (e.g. Bass and Torres Straits). On tide-dominated shelves the normalised bed shear stress time series is very similar on both the inner and outer shelf; characteristically periodic (Figure 4.6a and b). There may additionally be occasional episodic events in the shear stress time series at inner shelf sites that exceed the tidal contribution, due to the inner shelf being inside wave base and subject to infrequent tropical cyclones (Figure 4.6a). The frequency content of the

shear stress time series is similar for both the inner and outer shelf (Figure 4.6c); with the spectral energy associated with spring-neap tide cycles dominating. Relative spectral energy levels at other tidal frequencies are also similar across the full shelf width. Relative spectral energy levels at non-tidal frequencies, however, are much smaller on the outer shelf compared with the inner shelf. To summarise, on a tide-dominated shelf (a) seabed exposure is greatest in shallow water depths and in constrained seaways; and (b) spring-neap cycles cause the greatest variation in seabed exposure across the full shelf width.

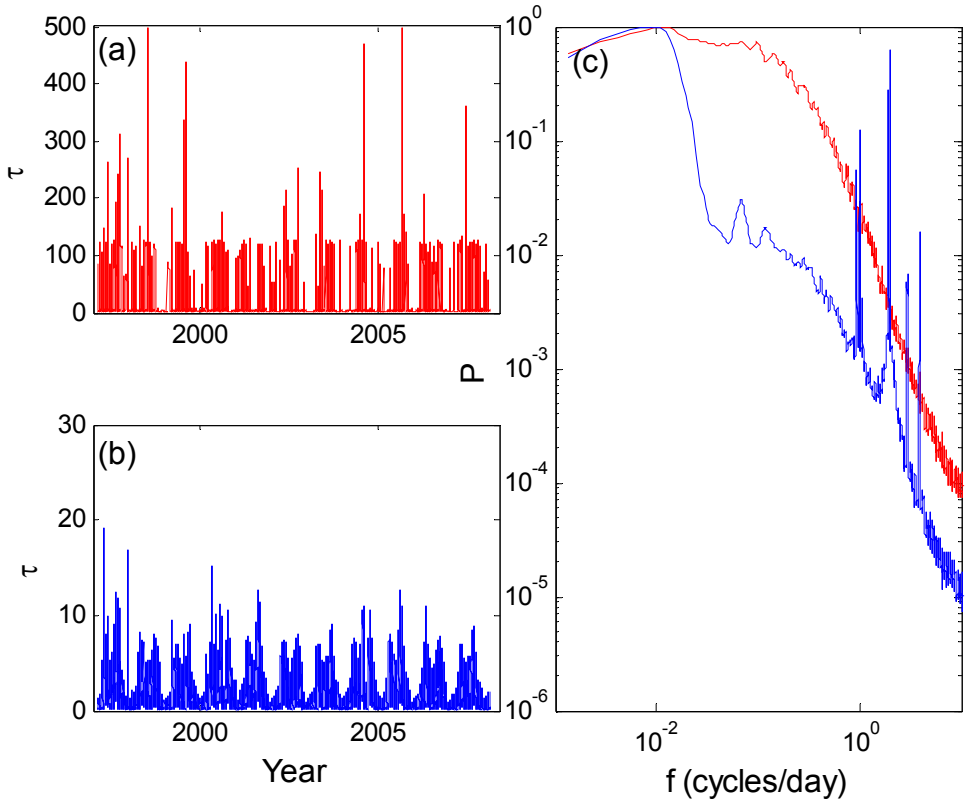

Figure 4.5: *Normalised (with respect to mean) bed shear stress time series on the (a) inner shelf and (b) outer shelf. The time series have been normalised against the median bed shear stress. (c) Normalised bed shear stress spectra for the inner (red) and outer (blue) shelf. Data are from the wave-dominated shelf (see Figure 4.3 and 4.4a) at 32.5°S 126.8°E (inner shelf, red) and 33.2°S 126.9°E (outer shelf, blue).*

Cyclone-dominated shelves are restricted to the tropical latitudes of northern Australia, thus in the absence of cyclones these shelves would most likely be tide-dominated or dominated by locally-generated seas (typically by the SE Trade Winds). In the latter case the wave period is short so that wave base is typically shallow (<30 m). The average picture for a cyclone-dominated shelf therefore mostly resembles a tide-dominated shelf (cf. Figure 4.4b and c). The magnitude of the average bed

shear stresses between these two examples differs, because one region is macrotidal and the other is meso-tidal, but the spatial pattern of variability is similar. Not surprisingly the normalised bed shear time series and spectrum from a cyclone-dominated shelf resembles a mixture of both tide-and wave-dominated shelves. The time series on the outer shelf displays mostly tidal characteristics because it is outside wave base, whereas the inner shelf time series is clearly tidal but punctuated by episodic cyclone events due to its location inside wave base (cf. Figures 4.7a and b). For the inner shelf the spectral energy is greatest at inter-annual frequencies, related to cyclone events, whereas on the outer shelf it is associated with the semi-diurnal tidal. There is a spectral peak at the spring-neap tide frequency, but the higher frequency tidal signals on the inner shelf are indistinguishable from wave events occupying a similar frequency band.

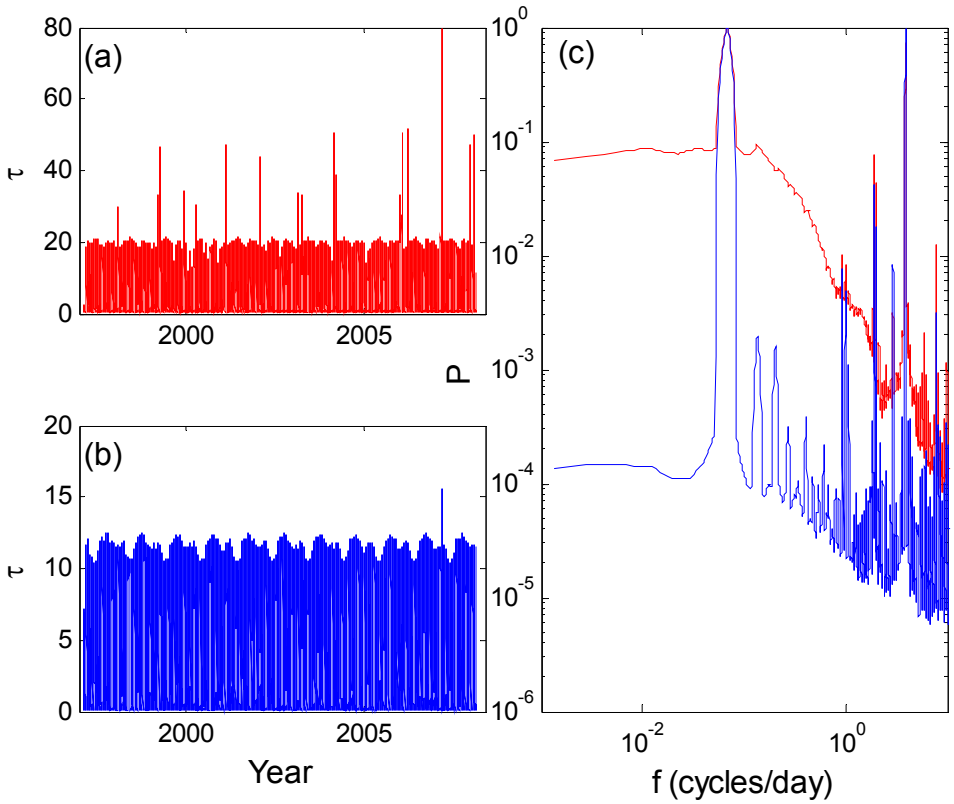

Figure 4.6: *Normalised bed shear stress time series on the (a) inner shelf and (b) outer shelf. The time series have been normalised against the median bed shear stress. (c) Normalised bed shear stress spectra for the inner (red) and outer (blue) shelf. Data are from the tide-dominated shelf (see Figure 4.3 and 4.4a) at 19.4°S 120.4°E (inner shelf, red) and 18.0°S 119.6°E (outer shelf, blue).*

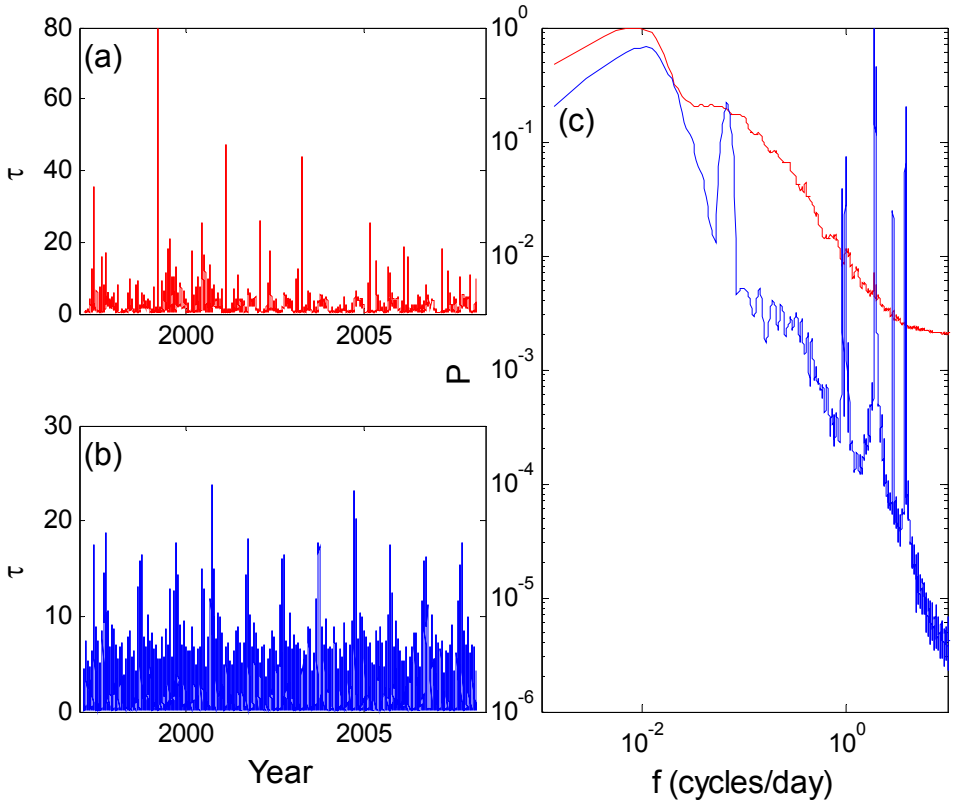

Figure 4.7: *Normalised bed shear stress time series on the (a) inner shelf and (b) outer shelf. The time series have been normalised against the median bed shear stress. (c) Normalised bed shear stress spectra for the inner (red) and outer (blue) shelf. Data are from the cyclone-dominated shelf (see Figure 4.3 and 4.4a) at 21.5°S 114.7°E (inner shelf, red) and 21.3°S 114.5°E (outer shelf, blue).*

5. Results – Potential surrogates for ecological disturbance

5.1 INTRODUCTION

Two key physical parameters that are inferred to be of critical importance for the creation of disturbed patches of habitats and the establishment of a disturbance regime are: a) the threshold magnitude; and b) the recurrence interval of threshold-exceeding bed shear stress events. For the threshold magnitude component (reviewed in Section 2.4), a Shield's parameter (non-dimensional bed shear stress) value of 0.25 is assumed to be the threshold for creating patches. This value is several times larger than that required to initiate traction bedload transport (~0.05) and falls in the middle of the ripple and dune bedform stability field. It represents conditions when the seabed is highly mobile (Figure 2.8) and where patches of disturbed habitat are likely to be created.

The recurrence interval of threshold-exceeding (patch creating) bed shear stress events is considered here in relation to the ecological succession (*ES*) rates for different substrates (Figure 2.3). Previous studies reviewed in Chapter 2 suggest that an optimised disturbance regime exists (and maximum biodiversity occurs) if patch creation occurs at a recurrence interval (*RI*) matching the community recovery time, which in turn is different for different substrate types (e.g. Newell et al., 1998; Fig. 2.3). Another aspect is the spatial scale of the patch-creating process and the size of patches of disturbed habitat created by an event. To account for spatial heterogeneity in both disturbance processes and substrate composition, we must define a spatial frame of reference and determine whether or not the patches of disturbed habitat created by an event are larger or smaller than the frame of reference. These concepts are fundamental to deriving any measure of habitat disturbance or the presence/absence of disturbance regimes. In order for the conditions of a true disturbance regime to be fulfilled, habitat patches of disturbed, recovering and equilibrium benthic communities must coexist within the spatial frame of reference. In other words, disturbance regimes only exist where the patches of disturbed habitat created by disturbance events occupy some fraction (*FA*) of the spatial frame of reference. Considering these factors together (Figure 5.1), we define here a dimensionless ecological disturbance index (*ED*), as the ratio of ecological succession and disturbance recurrence interval times the fraction of the area disturbed in any event:

$$ED = FA\frac{ES}{RI} \tag{5.1}$$

In the case where the frame of reference is equal to or less than the size of patches of disturbed habitat created by an event (*FA*=1) any event will result in the complete removal of the equilibrium community within the spatial frame of reference. This does not meet the criteria for a disturbance regime because habitat patches of disturbed, recovering and equilibrium benthic communities do not

coexist within the spatial frame of reference. Therefore, for a disturbance regime to exist, patches of disturbed habitat created by an event must be less than 100% of the frame of reference (*FA* must be fractionally less than 1).

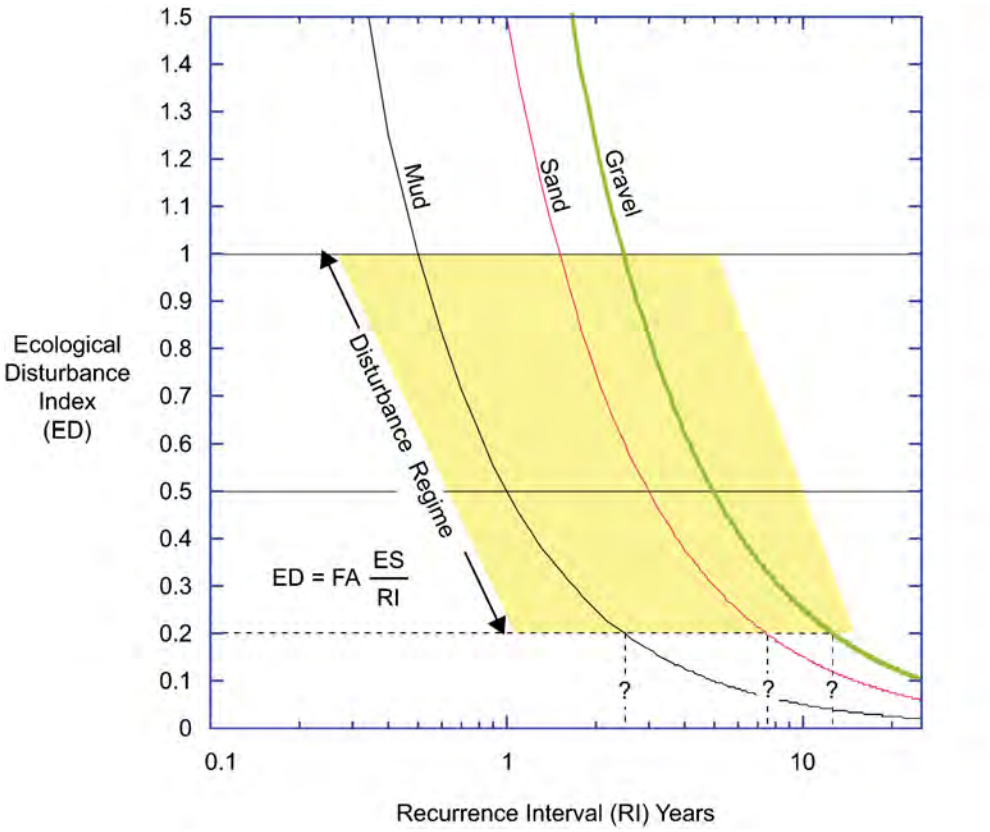

Figure 5.1: *Plot of Ecological Disturbance (ED) index for mud, sand and gravel versus the log of recurrence interval (RI) which is the average time in years between events where the Shield's parameter exceeds 0.25. We assume that these events attain sufficient shear stress magnitude to create a patch equal to 0.5 of the area of the chosen frame of reference (i.e. FA = 0.5). Small values of the ecological disturbance (ED) index represent decreasing proportions of time when disturbed/recovering habitats are present. ED>1 is out of range for disturbance regimes. The lower bound for disturbance regimes occurs when RI>>ES, assumed here to occur at ED ≈ 0.2. See text for further explanation.*

If the disturbance recurs at the same or lesser time intervals as the rate of ecological succession (one year for mud, 3 years for sand and 5 years for gravel; Section 2.3), then the effects of the disturbance are visible for 100% of the time and the conditions for a disturbance regime are not met. Where the recurrence interval is equal to the rate of ecological succession, the habitat will only just have completed its cycle of full recovery when the area within the frame of reference is disturbed again; the habitat occurring within the frame of reference is in a continuous state of recovery from disturbance and there is never an equilibrium community present. Hence, for conditions where

ES>*RI* (i.e. *ED*>1), the system is outside the limits of a disturbance regime as defined in this study (Figure 5.1).

At longer recurrence intervals of disturbance the equilibrium community is present within our frame of reference together with recovering habitat patches. For example, at twice the time required for ecological succession, we expect the disturbed habitat with pioneers to be present for 50% of the time and the equilibrium community to be present for 50% of the time. Recurrence intervals of disturbance equal to three or four times the time required for ecological succession result in decreasing proportions of time when the effects of disturbance are visible (33% of the time and 25% of the time, respectively). At increasing recurrence intervals it can be seen that *ED* is asymptotic to the X-axis, so *ED* does not reach zero. At some (small) value of *ED*, however, the proportion of time that disturbed/recovering communities are present is very small compared with the amount of time that the equilibrium community is present and we might agree that the recurrence interval is too large to have any significant influence on the "normal" state of the community. We acknowledge this is an arbitrary boundary, but suggest *ED*≈0.2 is a reasonable lower limit (Fig. 5.1). This equates with maximum recurrence intervals of around 2.5 years for mud, 7.5 years for sand and 10.5 years for gravel (Figure 5.1).

A theoretical maximum in biodiversity will occur for *ED*=0.5, where the patch areas cleared by one or more disturbances are equal to half the area of the frame of reference. This yields equal areas of equilibrium community and disturbed/recovering patches being present at any given time. We suggest that the relative proportion of different community areas affects community-biodiversity in the same way as the numbers of individuals affects the Shannon species-biodiversity index: a sample of 100 individuals comprised of 50 of species X and 50 of species Y is more diverse than a sample containing 99 of species X and only 1 of species Y. So a frame of reference of 100 km^2 comprised of 50% of equilibrium community and 50% of pioneer community is more diverse than one comprising 99% of equilibrium community and 1% of pioneer community.

The effect of including the spatial fraction multiplier (*FA*) in Equation 5.1 is to push the curves closer to the origin. This mathematical analysis ignores many complexities associated with the true heterogeneity of the seafloor which in turn, gives rise to habitat patchiness. During a shear stress event where the Shield's parameter exceeds 0.25, a number of factors may cause some areas to become quickly stripped clear of epibenthos and others to resist damage. These factors include subtle variations in depth, local shielding behind rocky outcrops, greater or lesser efficient biological or chemical bounding of bed sediments, bedform size and migration rates, sediment armouring of the bed and variations in the thickness (and availability for transport) of unconsolidated sediments.

In this study, our frame of reference is set by the model grid size equal to 0.1° (approximately 10 km by 10 km). This area (100 km^2) is clearly small compared with the size of oceanographic processes that might disturb the seafloor, such as tropical cyclones, temperate storms or intruding ocean currents. However, due to the factors listed above, we also know that 100 km^2 of seafloor is likely to possess a certain degree of heterogeneity that would result in a spatially patchy response to any disturbance event. We are not aware of any research that has measured the actual patchiness of disturbed benthic habitat resulting from a specific disturbance event. Therefore we have used assumed values of *FA* less than unity for the purposes of this study, meaning that any disturbance event will remove some (FA) fraction of the equilibrium community within each 100 km^2 grid cell.

5.2 NATIONAL OVERVIEW

In order to calculate the ecological disturbance index (*ED*), information is needed for the relevant component variables (Table 5.1). This includes information on the percentage of time that the Shields parameter θ >0.25, and the mean number of days between events when θ >0.25. We also consider a representation that is analogous to the work rate (*R*) of disturbing the seabed, given by:

$$R = \frac{\int_0^{t_{max}} \theta_{>0.25}.dt}{\int_0^{t_{max}} \theta.dt} \tag{5.2}$$

where t is time, t_{max} is the length of the time series, θ is the Shield's parameter, and $\theta_{>0.25}$ is that part of the Shield's parameter time series where the values exceed 0.25 (cf. Equation 4.1).

Table 5.1: List of parameters used to describe the disturbance regimes on the Australian shelf.

ITEM NO.	PARAMETER	ITEM NO.	PARAMETER
1	% time θ>0.25	3	Mean number of days between events
2	*R* (Eq. 5.2)	4	*ED* index (Eq. 5.1)

The procedure to determine the *ED* index at each location on the GEOMACS grid first involved classifying the bed sediment using a simple classification scheme of gravel, sand or mud. Grid cells were assigned to the gravel class if percent gravel was >30, and if the percent gravel was <30 they were assigned to either the sand or mud class depending on which ever had the largest percentage (cf. Folk, 1974; Fig. 5.2). The *ED* index was then calculated using Equation 5.1 and the appropriate value for *RI* depending on the sediment class (Section 5.1). Note that due to uncertainty surrounding the correct value of *FA* it was assigned a value of unity, thus we present values for *ED* up to 10 since they may be valid if *FA* assumes values as low as 0.1.

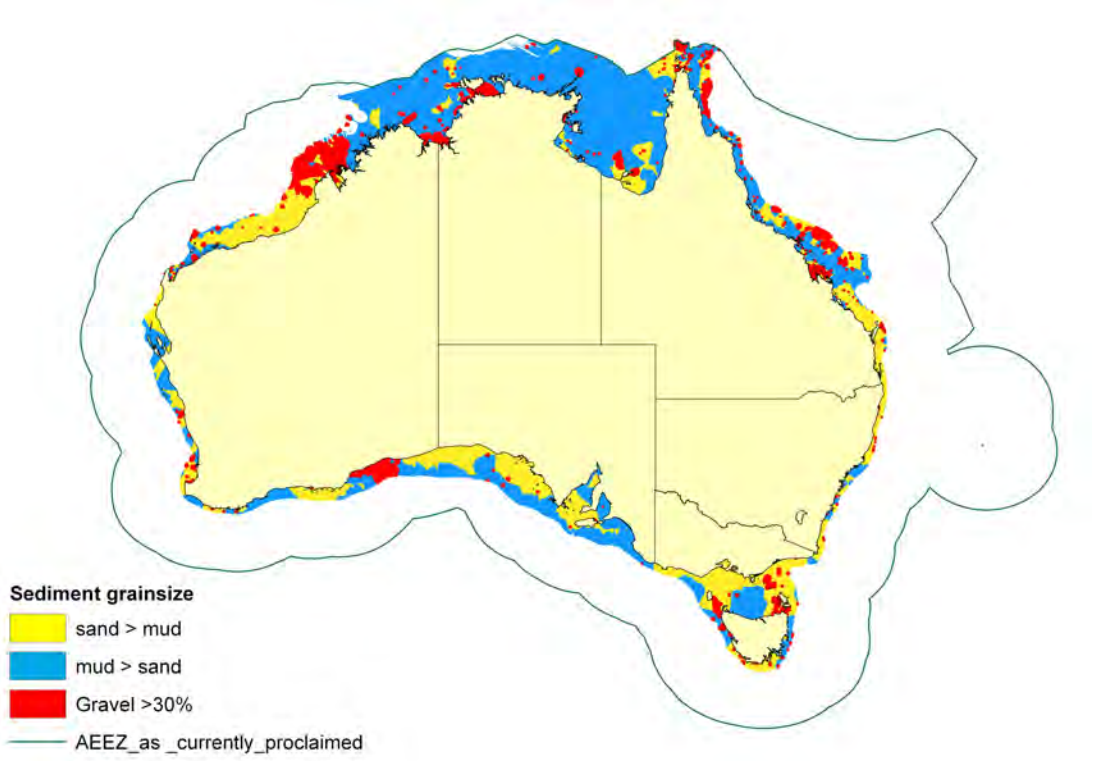

Figure 5.2: *Map showing the areas of gravel, sand and mud on the Australian continental shelf, derived from point measurement data stored in Geoscience Australia's MARS marine sediment database (http://www.ga.gov.au/oracle/mars/index.jsp).*

The range in magnitude of each parameter listed in Table 5.1 is large at the national scale. Frequency distributions of the spatial variability in each are shown in Figure 5.3, and they are also characteristically right-skewed. In order to highlight variability in the data, maps showing spatial variation in the parameters calculated to represent ecological disturbance have been log-transformed, with the exception of the *ED* index (Appendix B).

Largest values in percentage of time the Shield's parameter exceeds 0.25 occur across almost the entire shelf width in the north, whereas in the south largest values are constrained to the inner shelf (Figure B.1). The spatial pattern in this parameter is consistent with a tide-dominated northern half and wave-dominated southern half of the Australian Shelf. The spatial distribution of R (Eq. 5.2) is also consistent with the geographic extent of the disturbance drivers (i.e. waves and tides), but the relative range in values is more subtle (Figure B.2). The spatial pattern in mean number of days between events that the Shield's parameter exceeded 0.25, and the *ED* index, are shown in Figures B.3 and B.4 respectively. Note that areas that are shown as white on the shelf represent situations where there were less than 3 threshold exceeding events in the 11 year time series. An interpretation of these parameters is presented in the following section.

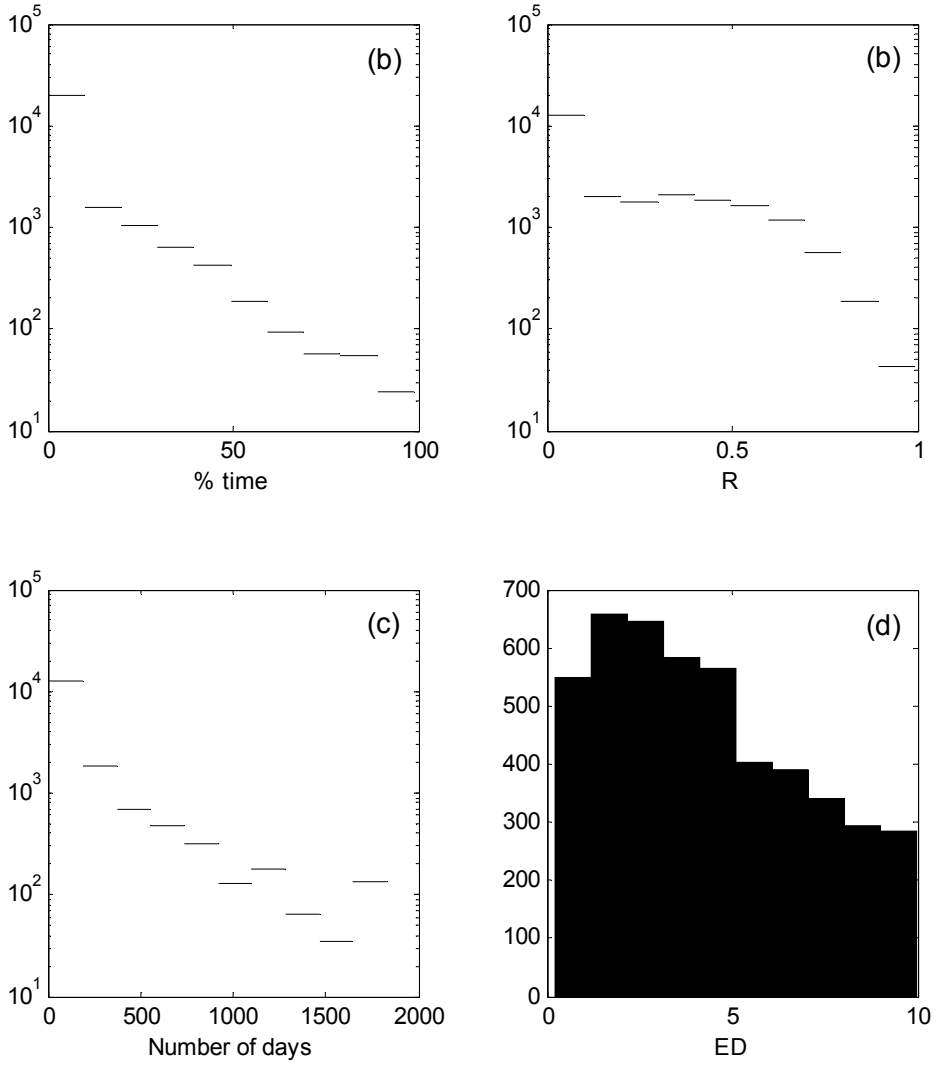

Figure 5.3: *Histograms (presented as number of grid cells) of: (a) Percentage of time θ>0.25; (b) R (Eq. 5.2); (c) mean number of days between events where θ>0.25; and (d) ED index (calculated using FA=1).*

5.3 REGIONAL EXAMPLES

To assist with interpretation of the national scale maps presented in Appendix B the three regions identified previously to exemplify wave- tide- and cyclone-dominated shelves are discussed again here (Figure 5.4). The shelf extent that each of these examples represents can be determined by comparing with Figure 2.10. On the wave-dominated shelf the mean number of days between threshold events that the Shield's parameter exceeds 0.25 is several hundred days on the outer shelf. On the inner shelf, and particularly close to the coastline, the number of days decreases to tens of days or less. This spatial pattern mirrors the bathymetry and exposure to the prevailing swell

direction; i.e. the minimum recurrence period between events is in the shallowest water depths and the coastal locations most exposed to the swell. In effect Figure 5.3a is the inverse of Figure 4.4a.

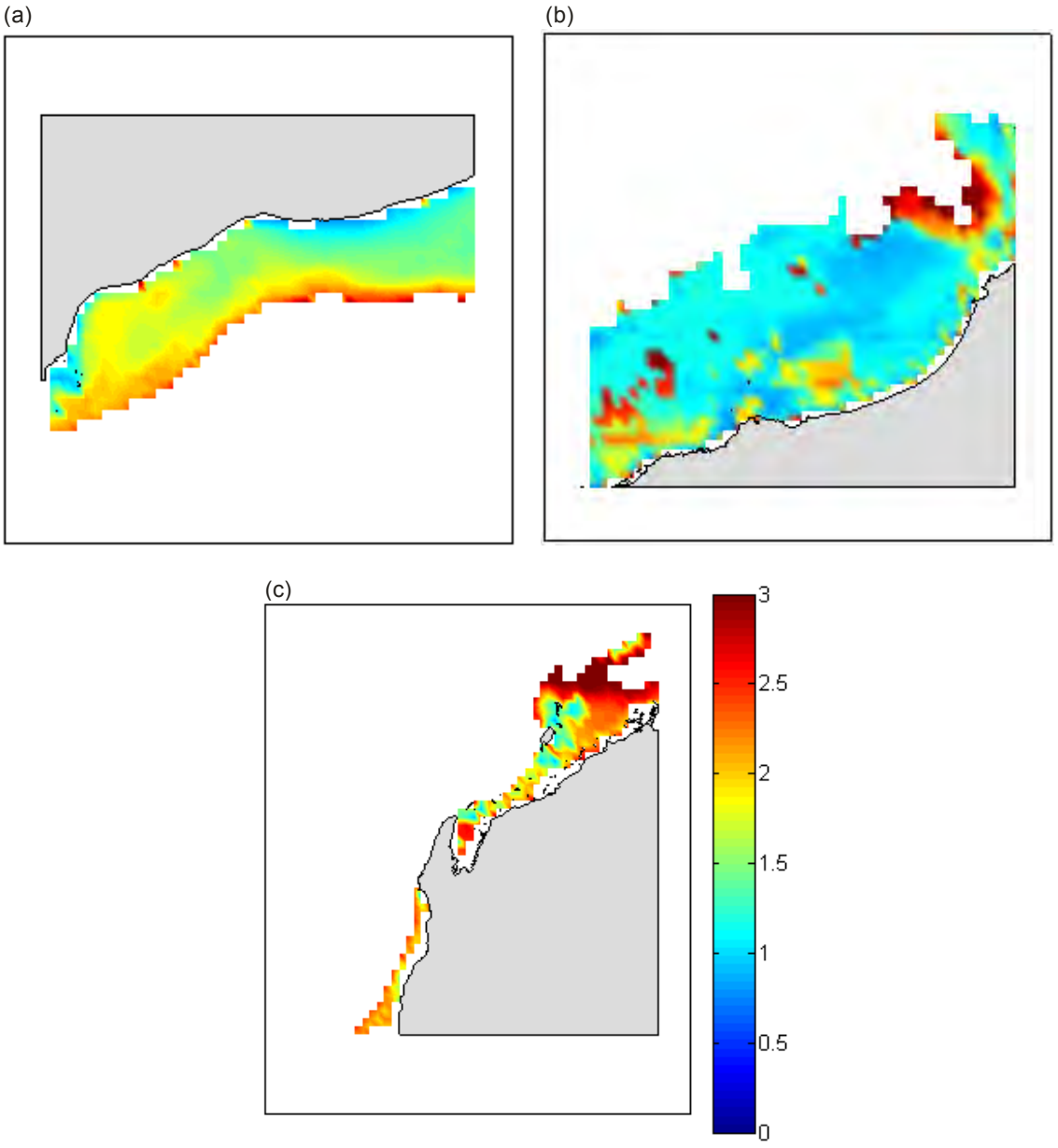

Figure 5.4: *Logarithm of the mean number of days between events where the Shield's parameter exceeds 0.25. The examples shown are for a (a) wave-dominated shelf, (b) tide-dominated shelf, and (c) cyclone-influenced shelf. The location of each region is shown on Figure 4.3.*

On the tide-dominated shelf the recurrence interval between threshold events is broadly consistent across the shelf width, of the order 10 days or more, and most likely tied to spring-neap tide cycles. Where the recurrence interval locally reaches one hundred to several hundred days the pattern in Figure 5.3b is not the inverse of that in Figure 4.4a. For example, there is an area in the northwest of

the region where the recurrence period between threshold events is of the order 1000 days, or more where the pixels are white. Yet this same area does not have the smallest mean bed shear stresses (cf. Figure 4.4b). It is, however, an area where the shelf is deeper than elsewhere and therefore more protected from the influence of wave events in the region. On a tide-dominate shelf, therefore, if the recurrence period between threshold events does not match a tidal period (e.g. semi-diurnal, diurnal or spring-neap), then it probably matches the wave regime.

On the cyclone-dominated shelf the recurrence period between threshold events is of the order several hundred to a thousand days across the entire shelf (Figure 5.4c). Where it is at the lower end of this range, south of Northwest Cape (Figure 5.4c), seasonal swell from the southern Indian Ocean probably also contributes to the disturbance regime. In the northern part of the region, and in Exmouth Gulf (Figure 5.4c), the threshold Shield's parameter is most likely only exceeded during cyclones. Cyclones impact this region on average 2.5 times a year, but the effects at any particular location are likely to be felt less frequently, depending on the precise track of the cyclone across the region.

The leap from number of days between threshold events of the Shield's parameter and the *ED* index is based on the seabed type (mud, sand and gravel) and the idealised ecological recovery rates associated with these seabed types (Fig. 5.1; Equation 5.1). Figure B.4 shows that for the threshold Shield's parameter and index functions chosen here (θ>0.25 and Figure 5.1) most of the Australian shelf has near-zero or unrecognised (>10) *ED* index values. On the southern wave-dominated shelf *ED* values indicative of a disturbance regime (any value up to 10 given that we have assumed for pragmatic reasons *FA*=1) occur almost exclusively at outer shelf water depths where infrequent, very high magnitude events occur with a recurrence period matching the optimum for the local seabed sediment type (Figures 5.5a and B.4). On the northern, tide-dominated shelf *ED* values indicative of a disturbance regime occur at the particular water depth range in which the threshold Shield's parameter is not exceeded by tides, but is exceeded by less frequent wave events whose recurrence period matches the optimum for the local seabed sediment type (Figures 5.4b and B.4). On cyclone-influenced shelves *ED* values indicative of a disturbance regime again occur for a range of water depths where the cyclone recurrence interval is optimal for the sediment type present (Figures 5.4c). Clearly the pattern in *ED* index values is highly sensitive to the chosen threshold Shield's parameter value and the local seabed type.

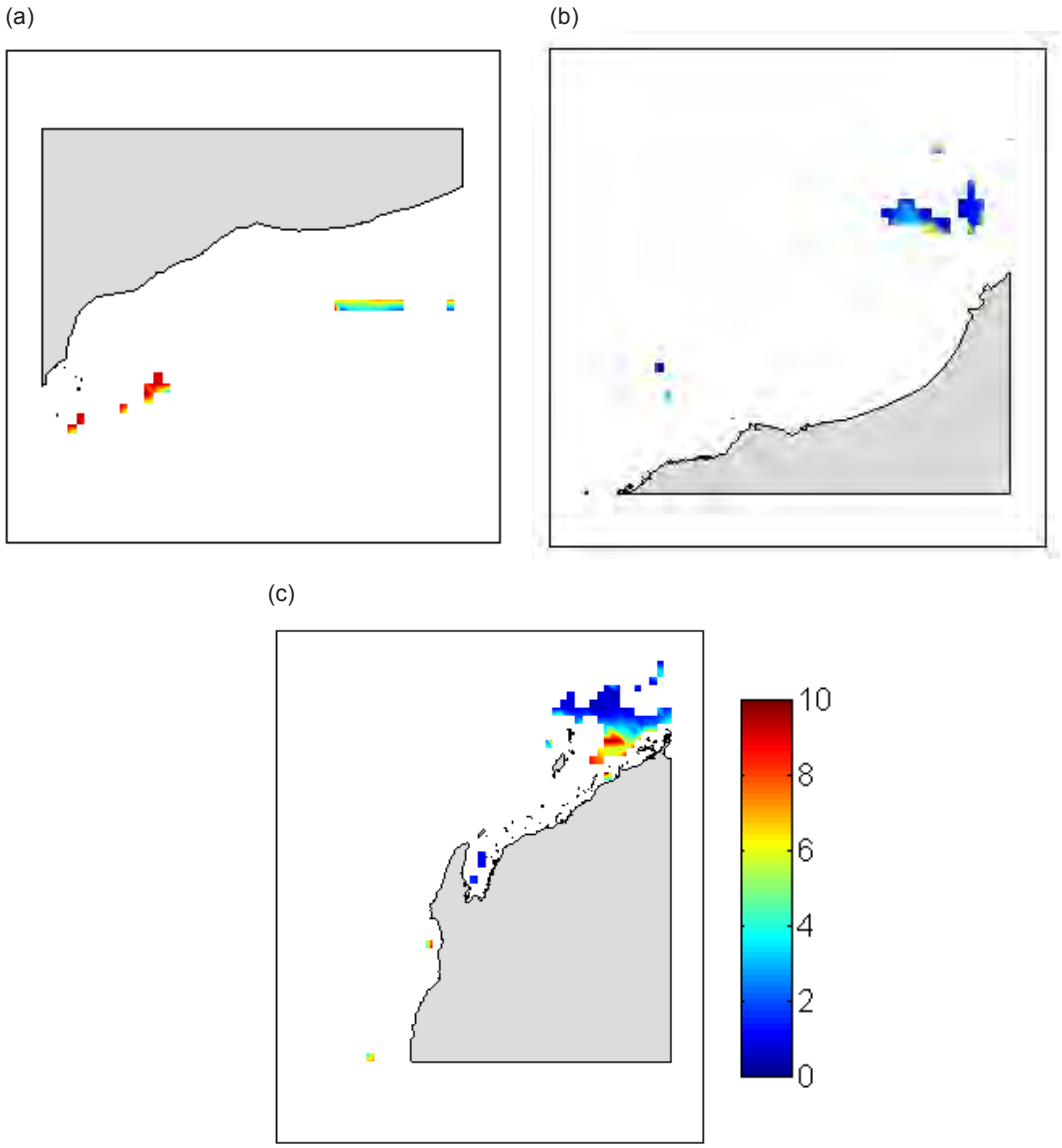

Figure 5.5: *ED index calculated for example areas (a) wave-dominated shelf, (b) tide-dominated shelf, and (c) cyclone-influenced shelf. The location of each region is shown on Figure 4.3. The map of ED calculated for the whole of Australia is shown in Appendix Figure B4.*

6. Discussion

6.1 LIMITATIONS OF THE MODEL DATA

The analysis presented here is based entirely on the predictions of a numerical model that provides bed shear stress time series across a spatial grid with a cell size of 0.1° square, and samples of sediment texture interpolated onto the same spatial grid. The following limitations apply to the data and derived parameters.

1. The modelled bed shear stress due to waves, tides and ocean currents has not been validated against field measurements in any way. Relative magnitudes across the spatial domain are expected to be correct, but the validity of actual magnitudes is unknown. This is problematic given that some of the analysis relies on actual magnitudes. For example, a non-dimensional bed shear stress of 0.25 is a critical magnitude.
2. Sediment texture information from available physical samples is inconsistent across the spatial domain and in many areas samples are sparse. Interpolated values for some grid cells is based on very few or no samples within the grid cell. Furthermore, it has been assumed here that the Folk classification scheme appropriately represents the benthic community's sediment texture preference. For example, percent gravel exceeding 20% was used to classify the seabed as gravel, but gravel-associated benthos may occupy wider or narrower ranges of percent gravel.
3. There is no available data base for rock coverage on the Australian shelf, so this seabed type and its associated benthos are unrecognised, and therefore have effectively been folded into the interpolated sedimentary seabed types. Around 5% of the Great Barrier Reef shelf area is expected to be coral limestone reef-rock (Hopley et al., 2007) and the rocky-reef areas of Australia's shelf were mapped by Heap and Harris (2008), but otherwise there are few reliable estimates available.
4. The ecological succession timescales for the various sediment types are based on studies in coastal settings (estuaries and bays) and their validity in shelf environments is unknown.

As a consequence of the above limitations it is recommended that parameters used to represent seabed exposure be normalised before using them in predictive models for biodiversity. The accuracy of the modelled bed shear stress has an important impact on the ecological disturbance (*ED*) index. If the modelled stresses are over- or under-estimated then our theoretically argued critical value of $\theta > 0.25$ is compromised. *ED* values outside the theoretically argued range (i.e. >1 and << 0.2) may therefore be valid indicators of a disturbance regime. Here we suggest that if *FA* is

assigned a value of unity then values of *ED* as great as 10 or as small as 0.1 may be indicative of a disturbance regime. Acceptable values indicative of a disturbance regime may actually be larger.

6.2 EXPOSURE AND DISTURBANCE

Our approach has been to focus attention on the exposure of the seabed to physical, patch-clearing processes that may cause the dislodgement or burial of animals by sediment transport. To a first approximation, the map in Figure B4 indicates those parts of the Australian continental shelf where, by our estimation, the conditions are met for wave and current-induced physical disturbance regimes to exist. However, our analysis does not extend to other, more subtle physical disturbances that may create patches of disturbed habitat. For example, a slight increase in turbidity can block sunlight to benthic plants that survive at the limits of the photic zone on a minute quantity of radiation. Small increases in suspended sediment concentration might clog the sensitive filter feeding mechanisms of sessile animals adapted to very low levels of suspended matter. Bedload transport need not bury an animal to kill it; the abrasion caused by moving sediment might be sufficient to weaken an animal's resistance to parasites or diseases under certain conditions. Furthermore, it is acknowledged that exposure to seabed shear stress may be combined with other parameters, such as changes in temperature, salinity or nutrient loads all affected by a single storm event (for example). Thus, even where the seabed stress levels do not exceed a Shields parameter threshold of 0.25, a combination of factors could possibly kill benthic animals in a particular location and there are many possible ways that physical disturbances can have the result of creating vacant habitat patches which are not accounted for in our analysis.

The potentially innumerable combinations of different processes that might cause a patch-clearing disturbance event will expand the areas depicted in Figure B4. The converse situation, where the exceedence of a Shields parameter threshold of 0.25 does not cause sediment mobilisation and dune migration, could theoretically occur where the bed is armoured, where sediments have been chemically or biologically bound or where rock is exposed on the seabed. Recalling that a Shields parameter threshold of 0.25 equates with bed stress of sufficient magnitude to induce bedform migration in medium to coarse sand, which is far in excess of the bed stress required to initiate bedload transport for a grain diameter in the medium sand range ($D_* \approx 10-20$) (i.e. a Shields parameter $\theta_c \approx 0.05$) we suggest that our spatial analysis of ED (Figure B4) provides a conservative first approximation within the constraints of the GEOMACs model.

As was alluded to in the introduction to this report, our analysis addresses only physical disturbance of the benthos and ignores biotic (e.g. predation, nutrient availability), chemical (e.g. dissolved oxygen, pH), and anthropogenic agents among others. In this way, our analysis of ED (Figure B4) is

again conservative, in as much as the additional potential disturbance agents are potentially contemporaneous and additive in their capacity to create patches of disturbed habitat.

6.3 FUTURE WORK

There are a number of possible avenues that future work could pursue to improve the reliability of spatial predictions of ED as well as validation of the ecological response to the impacts of various disturbance agents over a range of spatial and temporal scales. Here we list a few likely areas where we believe further work may have the greatest impact on understanding physical disturbance regimes on Australia's continental shelf, namely: a) improved modelling of physical processes; b) better understanding of ecological recovery rates for different habitats; and c) a better understanding of the spatial scales associated with different disturbance processes.

In order to improve the reliability of the GEOMACS model for estimating bed stress on the Australian shelf, improvement of the GEOMACS tidal model and coupling of the ocean current time series with waves and tides would make the greatest improvement. The tidal model suffers from lack of calibration in several locations and it was based on the 2001 version of the GA bathymetry grid, which has subsequently been revised and updated (Whiteway, 2009). Revising and updating the tidal prediction component of GEOMACS will improve the quality of bed stress predictions particularly in the macrotidal regions of Australia. Even more useful would be obtaining coincident OCCAM or BlueLink ocean current model output for the period of the GEOMACS wave and tide time series. This would greatly improve the accuracy of estimated bed stress levels through appropriate phasing of the process drivers. Finally, in order to resolve a better record of cyclone events a longer time series (> 50 years) would be desirable.

A limiting factor in modelling the physical processes is the quality of underlying information on seabed properties in terms of the distribution of samples with reliable grain size measurements, plus the inclusion of a rock/sediment qualifier. In some areas, such as the shelf adjacent to the Kimberly region of Western Australia, there are no measurements of seabed sediment grain size. Also, the rock/sediment qualification of seabed type is a fundamental, first-order discriminator in benthic ecology and its inclusion would greatly enhance the value of the modelling work.

Knowledge of ecological recovery rates for different habitats types is lacking for most shelf environments and this has obvious implications for our ability to assess ecological disturbances (Fig. 5.1; Equation 5.1). Such knowledge is not only of interest to the disturbance modelling work presented here, but it is also vital to managers tasked with responding to anthropogenic

environmental incidents like the Montaro petroleum well blowout on the North West Shelf in 2009. Any information on ecosystem recovery rates on Australia's shelf (particularly in areas of intense industrial activity like the North West Shelf) would make a significant and valuable contribution to Australia's marine zone management needs.

The third issue we suggest requires attention is the lack of basic information on the spatial scales associated with different physical disturbance processes. That is, the length scale *FA* (Equation 5.1) has not been measured for any process (cyclones, ocean currents or temperate storms) for any shelf environment; to our knowledge, there has not been any research published on this topic. Although we might intuitively assign a length scale to the disturbances of cyclones or ocean current eddies having a measured radius wherein the seabed is exposed to a particular magnitude of stress, there is a paucity of direct observational evidence to document the spatial extent or degree of disturbance that has resulted from any specific discrete event. Field surveys designed to address this data gap are required before any further progress can be made in modelling physical disturbance processes including a reasonable estimate of the length scale *FA*.

7. Conclusions

Australia's marine conservation initiatives are designed to protect biodiversity by means of including information on habitats and ecosystem processes. As such, an understanding of the dominant disturbance-causing processes that define and characterise different benthic environments is an important factor to ensuring that the full range of different environments have been identified so that they can be included in the design of conservation measures. However, even though many specialists have recognised the importance of including disturbance among the ecosystem characteristics targeted for protection, there has not been a great deal of success to date in including them in design and management of marine protected areas. This is probably because our understanding of ecological disturbance is poor and our ability to represent disturbance processes spatially is limited.

The work presented in this report represents progress towards capturing the physical aspects of shelf disturbances based on sedimentological concepts, by providing methods to generate ecologically meaningful regionalisations. Our study has shown that it is feasible to model some of the key aspects of shelf disturbance, including the frequency and magnitude of disturbance in relation to seabed sediment size (gravel, sand or mud) and the source of disturbance (wave-dominated shelf, tide-dominated shelf or tropical cyclone dominated shelf). Our approach here was to exploit the link between modelled bed shear stress due to waves, tides and ocean currents and what is known about rates of ecological succession for different substrate types (gravel, sand, mud; Fig. 5.1) in order to derive maps predicting the spatial distribution of a dimensionless ecological disturbance index (*ED*), given as: $ED = FA\frac{ES}{RI}$

where *ES* is the ecological succession rate for different substrates, *RI* is the recurrence interval of disturbance events and *FA* is the fraction of the frame of reference disturbed. The map thus produced of *ED* for the Australian continental shelf shows small patches of seafloor distributed around the continent, on both the inner and outer shelf. Only a small portion of the shelf (perhaps ~10%) is characterised by a disturbance regime as defined here. Within these areas, the recurrence interval of disturbance events is comparable to the rate of ecological succession and meets our defined criteria for a disturbance regime. To our knowledge, this is the first time such an analysis has been attempted for any continental shelf.

In order to make further progress, we suggest attention should be focussed on: a) improved modelling of physical processes; b) better understanding of ecological recovery rates for different habitats; and c) a better understanding of the spatial scales associated with different disturbance

processes. Field studies of the spatial scale of physical disturbances caused by storms or intruding ocean currents on continental shelves are lacking and this is a major impediment to linking process studies to the design of spatial marine zone management tools. Finally, longer time-series records for disturbances are needed to characterise extreme storm events. It is important to remember that real-time estimates of disturbance "weather" are not essential, but rather information on the long term disturbance "climate" is needed. This could be derived using predictive climate models, supplemented by palaeo-climate records from coral, sediment and ice-core records.

8. References

Allen, J.R.L., 1985. *Principles of Physical Sedimentology*. George Allen & Unwin, 272 pp.

Allen, P.A., 1997. *Earth Surface Processes*. Blackwell Science, 404 pp.

Aller, J.Y., Todorov, J.R., 1997. Seasonal and spatial patterns of deeply buried calanoi copepods on the Amazon shelf: Evidence for periodic erosional/depositional cycles. *Estuarine, Coastal and Shelf Science,* 44 (1), 57–66.

Anderson, O.B., Woodworth, P.L., Flather, R.A., 1995. Intercomparison of recent global ocean tide models. *Journal of Geophysical Research* 100 (C12), 25,261-225,282.

Canals, M., Puig, P., de Madron, X.D., Heussner, S., Palanques, A., Fabres, J., 2006. Flushing submarine canyons. *Nature*, 444, 354-357.

Carruthers, T.J.B., Dennison, W.C., Longstaff, B.J., Waycott, M., Abal, E.G., McKenzie, L.J., Lee Long, W.J. (2002) Seagrass habitats of north-east Australia: models of key processes and controls. *Bulletin of Marine Science,* 71, 1153–1169.

Cheroske, A.G., Williams, S.L., Carpenter, R.C., 2000. Effects of physical and biological disturbances on algal turfs in Kaneohe Bay, Hawaii. *Journal of Experimental Marine Biology and Ecology,* 248 (1), 1–34.

Cogan, C.B., Todd, B.J., Lawton, P., Noji, T.T., 2009. The role of marine habitat mapping in ecosystem-based management. *ICES J. Mar. Sci.* 66 (9), 2033-2042.

Connell, J. H., 1978. Diversity in tropical rain forests and coral reefs. *Science,* 199, 1302-1310.

Connell, J. H., 1997. Disturbance and recovery of coral assemblages. *Coral Reefs,* 16, 101-113.

Daniell, J., Harris, P.T., Hughes, M., Hemer, M., Heap, A., 2008. The potential impact of bedform migration on seagrass communities in Torres Strait, Northern Australia. *Continental Shelf Research* 28, 2188-2202.

Done, T. J., 1992. Effects of tropical cyclone waves on ecological and geomorphological structures on the Great Barrier Reef. *Continental Shelf Research,* 12(7/8), 859-872.

Egbert, G.D., Bennett, A.F., Foreman, M.G.G., 1994. TOPEX/POSEIDON tides estimated using a global inverse model. *Journal of Geophysical Research* 99, 24821–24852.

Field, M. E., 2005. Living with change: response of the seafloor to natural events. *American Fisheries Society Symposium,* 41, 215-218.

Folk, R. L., 1974. *Petrology of sedimentary rocks*. Austin, Texas, Hemphills, 182 pp.

Gagan, M. K., Chivas, A. R. and Herczeg, A. L., 1990. Shelf wide erosion, deposition and suspended sediment transport during cyclone Winifred, central Great Barrier Reef, Australia. *Journal of Sedimentary Petrology,* 60(3), 456-470.

Grant, W. D. and Madsen, O. S. (1986) The continental-shelf bottom boundary layer. *Annual Review of Fluid Mechanics,* 18, 265-305.

Greenslade, D.J.M. 2001 The assimilation of the ERS-2 significant wave height data in the Australian region. *Journal of Marine Systems* ;28:141–60.

Halford, A., Cheal, A. J. , Ryan, D. and Williams, D. M., 2004. Resilience to large-scale disturbance in coral and fish assemblages on the Great Barrier Reef. *Ecology*, 85(7), 1892–1905.

Hall, S.J., 1994. Physical Disturbance and Marine Benthic Communities: Life in Unconsolidated Sediments. *Oceanography and Marine Biology: An Annual Review,* 32, 179–239.

Harmelin-Vivien, M. L., 1994. The effects of storms and cyclone on coral reefs: a review. *Journal of Coastal Research,* 12, 211-231.

Harris, P.T., 1992. *Dune migration in Australian seaways*. University of Sydney Ocean Sciences Institute Report 52, 60pp.

Harris, P.T., 1994. Comparison of tropical, carbonate and temperate, siliciclastic tidally dominated sedimentary deposits: examples from the Australian continental shelf. *Australian Journal of Earth Science* 41, 241-254.

Harris, P.T., 1995. Marine geology and sedimentology of the Australian continental shelf. In: Zann, L.P., Kailola, P. (Eds.), *The State of the Marine Environment Report for Australia Technical Annex 1*: The Marine Environment. Department of the Environment, Sport and Territories, Canberra, pp. 11-23.

Harris, P.T., 2010. On seabed disturbance, marine ecological succession and applications for environmental management: a physical sedimentological perspective. In: Li, M., Sherwood, C., Hill, P. (Eds.), *Sediments, Morphology and Sedimentary Processes on Continental Shelves*. International Association of Sedimentologists Special Publication, Blackwell Publishing Ltd, Oxford.

Harris, P.T., Smith, R., Anderson, O., Coleman, R., Greenslade, D., 2000. GEOMAT - *Modelling of Continental Shelf Sediment Mobility in Support of Australia's Regional Marine Planning Process*. Australian Geological Survey Organisation.59p.

Hasselman, K., (WAMDI Group), 1988. The WAM model - A third generation ocean wave prediction model. *Journal of Physical Oceanography* 18, 1775-1810.

Haywood, M.D.E., Browne, M., Skewes, T., Rochester, W., McLeod, I., Pitcher, R., Dennis, D., Dunn, J., Cheers, S., Wassenberg, T., 2007. *Improved knowledge of Torres Strait seabed biota and reef habitats.* Marine and Tropical Sciences Research Facility, Cairns, p. 115.

Hearn, C. J. and Holloway, P. E., 1990. A three-dimensional barotropic model of the response of the Australian North West Shelf to tropical cyclones. *Journal of Physical Oceanography*, 20, 60-80.

Heap, A. and Harris, P.T., 2008. Geomorphology of the Australian margin and adjacent sea floor. *Australian Journal of Earth Science* 55 (4), 555-584.

Hemer, M., 2006. The magnitude and frequency of combined flow bed shear stress as a measure of exposure on the Australian continental shelf. *Continental Shelf Research*, 26, 1258–1280.

Hemer, M.A., Church, J.A., Hunter, J.R., 2009. Variability and trends in the directional wave climate of the Southern Hemisphere. *International Journal of Climatology* 30 (4), 475-491.

Holpley, D., Smithers, S.G., Parnell, K.E., 2007. *The Geomorphology of the Great Barrier Reef: Development, Diversity and Change*. Cambridge University Press, Cambridge.

Hubbard, D. K., 1992. Hurricane-induced sediment transport in open-shelf tropical systems - an example from St. Croix, U.S. Virgin Islands. *Journal of Sedimentary Petrology*, 62, 946-960.

Huston, M., 1979. A general hypothesis of species diversity. *American Naturalist*, 113, 81-101.

Jones, A.T., Kennard, J.M., Ryan, G.J., Bernardel, G., Earl, K., Rollet, N., Grosjean, E., and Logan, G.A., 2007. *Geoscience Australia Marine Survey SS06/2006 Post-Survey Report: Natural Hydrocarbon Seepage Survey on the Central Northwest Shelf*. Geoscience Australia Record 2007/21.

Kantha, L.H., 1995. Barotropic tides in the global oceans from a nonlinear tidal model assimilating altimetric tides 1. Model description and results. *J. Geophys. Res*. 100 (C12), 25283– 25308.

Keen, T. R. and Slingerland, R. L., 1993. A numerical study of sediment transport and event bed genesis during Tropical Storm Delia. *Journal of Geophysical Research*, 98(3), 4775-4791.

Levitus, S., 1982. *Climatological atlas of the world ocean*. U.S. Dept. of Commerce, National Oceanic and Atmospheric Administration.

Li, M.Z., Amos, C.L., 2001. SEDTRANS96: the upgraded and better calibrated sediment-transport model for continental shelves. *Computers & Geosciences* 27 (6), 619-645.

Long, B., Bode, L., Mason, L. and Pitcher, C. R., 1997. Seabed current stress predicts the distribution and abundance of epibenthos in Torres Strait - *Report to Australian Fisheries Management Authority. Cleveland, Queensland, CSIRO Division of Marine Research.*

Lourensz, R.S., 1981. *Tropical Cyclones in the Australian Region July 1909 to June 1980*. Hedges and Bell Publ. Co., for the Australian Bureau of Meteorology, Maryborough, Victoria.

Lutjeharms, J. R. E., 2007. Three decades of research on the greater Agulhas Current. *Ocean Science*, 3, 129–147.

McLachlan, A., Jaramillo, E., Donn, T.E., Wessels, F., 1993. Sandy beach macrofauna communities and their control by the physical environment: a geographic comparison. *Journal of Coastal Research* 15, 27-38.

Mann, K. H. and Lazier, J. R. N., 2006. *Dynamics of Marine Ecosystems - Biological-Physical Interactions in the Oceans*. Blackwell Publishing, Oxford, 496pp.

Masselink, G., Hughes, M.G., 2003. *Introduction to coastal processes and geomorphology*. Hodder & Stoughton, London, 354 pp.

Morton, R. A., 1988. Nearshore responses to great storms. In: H. E. Clifton (ed), *Sedimentologic consequences of convulsive geologic events, Geological Society of America,* 229, 1-22.

Nielsen, P., 1992. *Coastal Bottom Boundary Layers and Sediment Transport*. World Scientific, 324 pp.

Newell, R. C., Seiderer, L. J. and Hitchcock, D. R., 1998. The impact of dredging works in coastal waters: a review of the sensitivity to disturbance and subsequent recovery of biological resources on the sea bed. *Oceanography and Marine Biology Annual Review*, 36, 127-178.

Nunes Vaz, R. A., Lennon, G. W. and Bowers, D. G., 1990. Physical behaviour of a large, negative or inverse estuary. *Continental Shelf Research*, 10(3), 277-304.

Passlow, V., Rogis, J., Hancock, A., Hemer, M.A., Glenn, K., Habib, A., 2005. *Final report - national marine sediments database and seafloor characteristics project.* Geoscience Australia Record 2005/8, Canberra.120p.

Pickett, S. T. and White, P. S., 1985. *The ecology of natural disturbance and patch dynamics*. Academic Press, London, 472pp.

Porter-Smith, R., Harris, P. T., Andersen, O. B., Coleman, R., Greenslade, D. and Jenkins, C. J., 2004. Classification of the Australian continental shelf based on predicted sediment threshold exceedance from tidal currents and swell waves. *Marine Geology*, 211, 1–20.

Proulx, M., Mazumder, A., 1998. Reversal of grazing impact on plant species richness in nutrient-poor versus nutrient-rich ecosystems. *Ecology* 79 (8), 2581-2592.

Puotinen, M. L., 2004. Tropical cyclones in the Great Barrier Reef, Australia, 1910–1999: a first step towards characterising the disturbance regime. *Australian Geographical Studies*, 42(3), 378–392.

Shields, A. 1936. Application of similarity principles and turbulence research to bed-load movement. *Mitteilunger der Preussischen Versuchsanstalt f˙ur Wasserbau und Schiffbau* 26: 5–24

Sleath, J.F.A., 1984. *Seabed Mechanics*. John Wiley & Sons, 335 pp.

Soulsby, R., 1997. *Dynamics of Marine Sands*. Thomas Telford, London.

Sousa, W.P., 1984. The role of disturbance in natural communities. *Annual Review of Ecology and Systematics* 15, 353-391.

Svensson, J.R., Lindegarth, M., Siccha, M., Lenz, M., Molis, M., Wahl, M., Pavia, H., 2007. Maximum species richness at intermediate frequencies of disturbance: consistency among levels of productivity. Ecology 88 (4), 830-838.

Thomsen, M.S., Wernberg, T., Kendrick, G.A., 2004. The effect of thallus size, life stage, aggregation, wave exposure and substratum conditions on the forces required to break or dislodge the small kelp Ecklonia radiata. *Botanica Marina*, 47(6), 454–460.

Tucker, M.E., 1995. *Sedimentary Petrology: An Introduction to the Origin of Sedimentary Rocks*. Blackwell Science.

Van Woesik, R., Ayling, A. M. and Mapstone, B., 1991. Impact of tropical cyclone 'Ivor' on the Great Barrier Reef, Australia. *Journal of Coastal Research*, 7(2), 551-558.

Warwick, R.M. and Uncles, R.J., 1980. Distribution of benthic macrofaunal associations in the Bristol Channel in relation to tidal stress. *Marine Ecology Progress Series,* 3, 97–103.

Webb, D.J., Cuevas, B.A., Coward, A.C., 1998. *The first main run of the OCCAM global ocean model. Internal Report of James Rennell Division*, Southampton Oceanography Centre, UK, 50pp. See also: http://www.noc.soton.ac.uk/JRD/OCCAM

Whiteway, T., 2009. *Australian bathymetry and topography grid*. Geoscience Australia Record 2009/21, Canberra, p. 51.

Williams, G. D. and Bindoff, N. 2003. Wintertime oceanography of the Adelie Depression. *Deep Sea Research Part II,* 50(8-9), 1373-1392.

Wu, J., Loucks, O.L. 1995. From balance of nature to hierarchical patch dynamics: a paradigm shift in ecology. *The Quarterly Review of Biology*, 70 (4), 439-466.

Appendix A

Maps of parameters representing benthic exposure on the Australian shelf

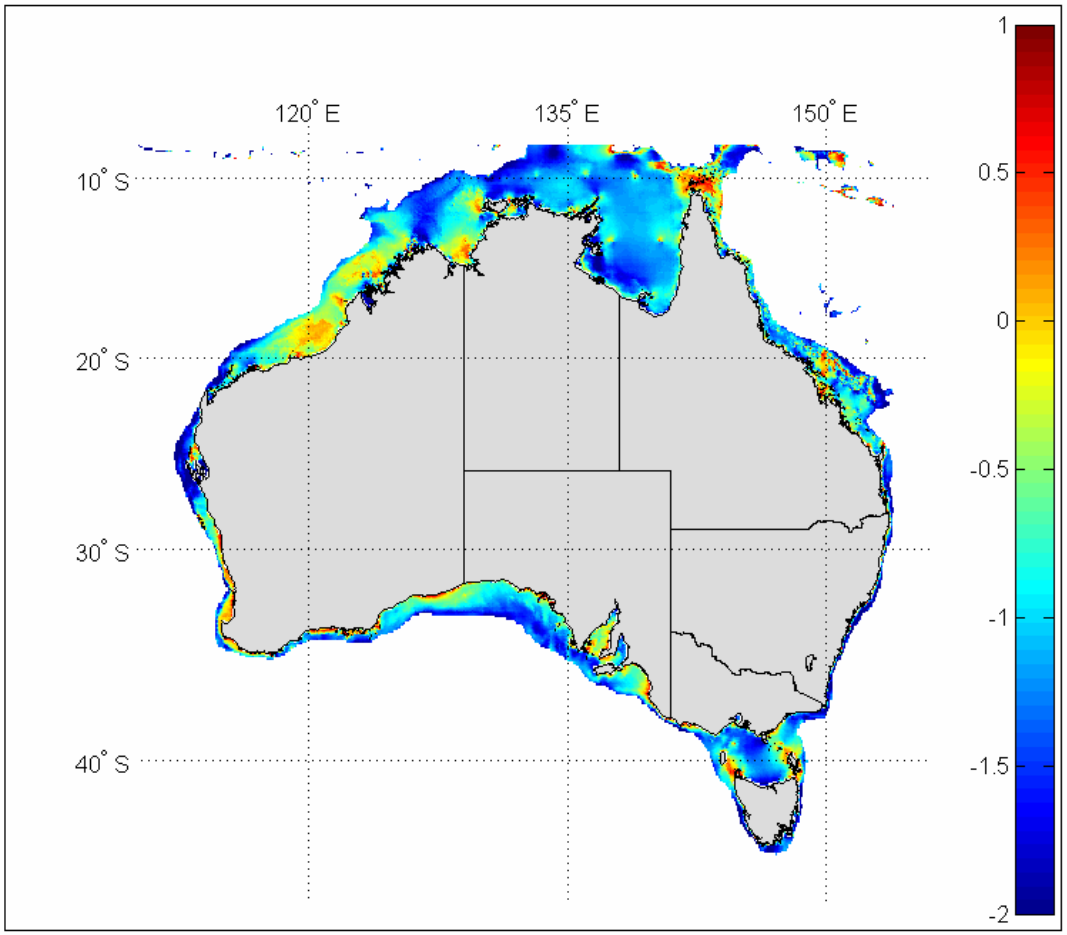

Figure A.1: Map showing logarithm of the mean bed shear stress (Nm^{-2}) on the Australian shelf.

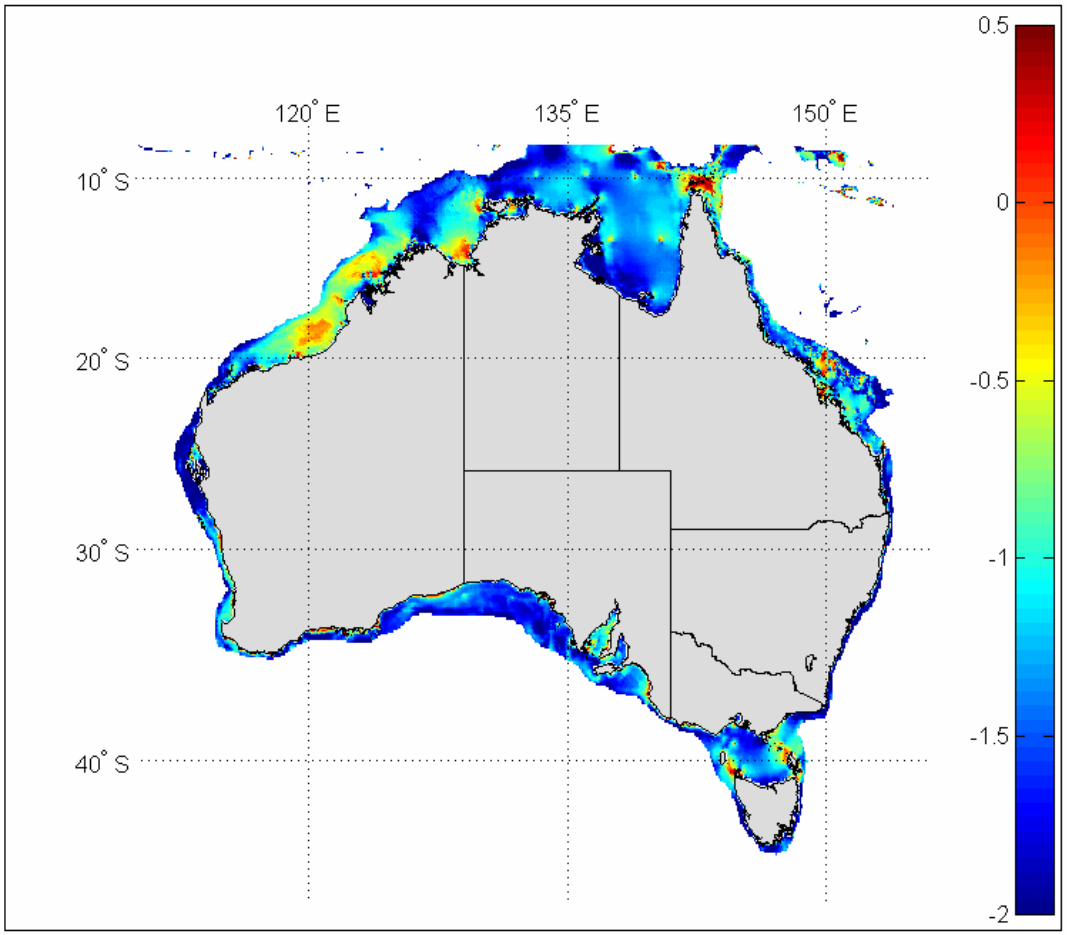

Figure A.2: Map showing logarithm of the trimmed mean bed shear stress (Nm^{-2}) on the Australian shelf.

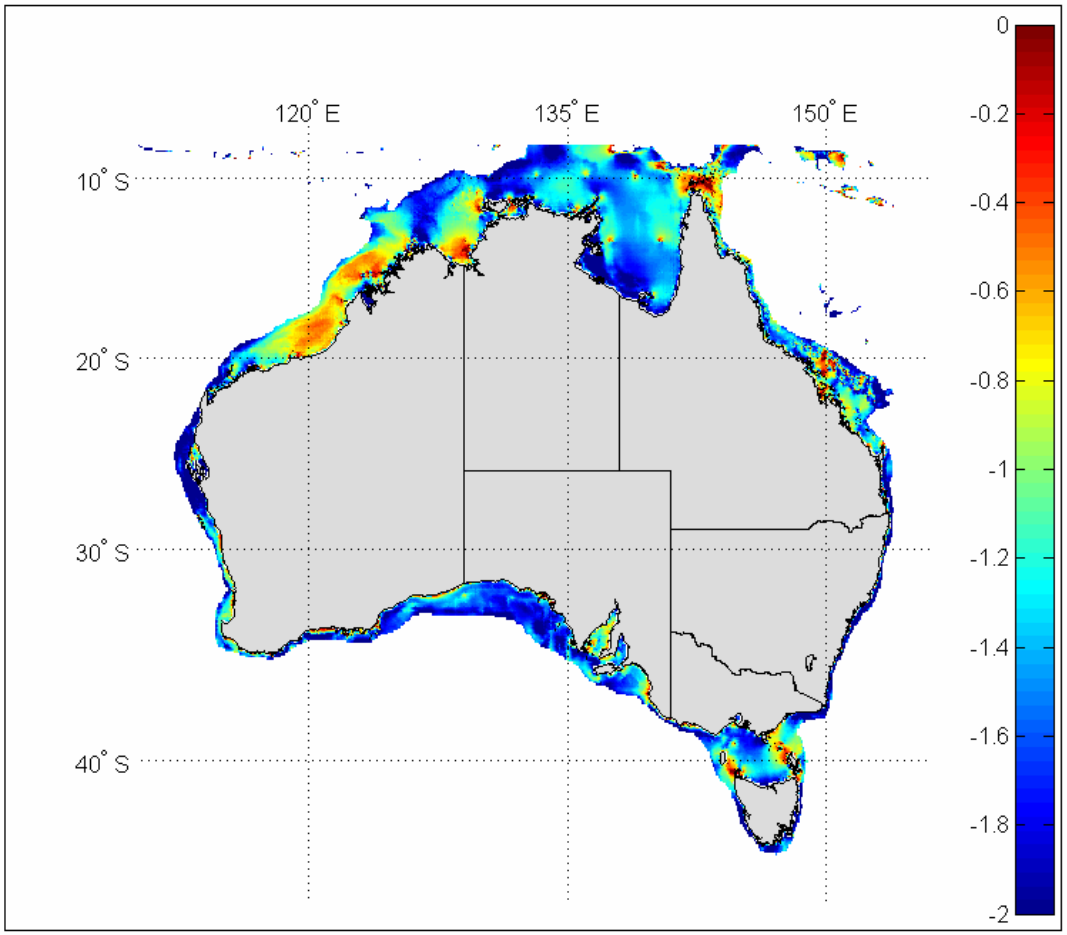

Figure A.3: Map showing logarithm of the median bed shear stress (Nm^{-2}) on the Australian shelf.

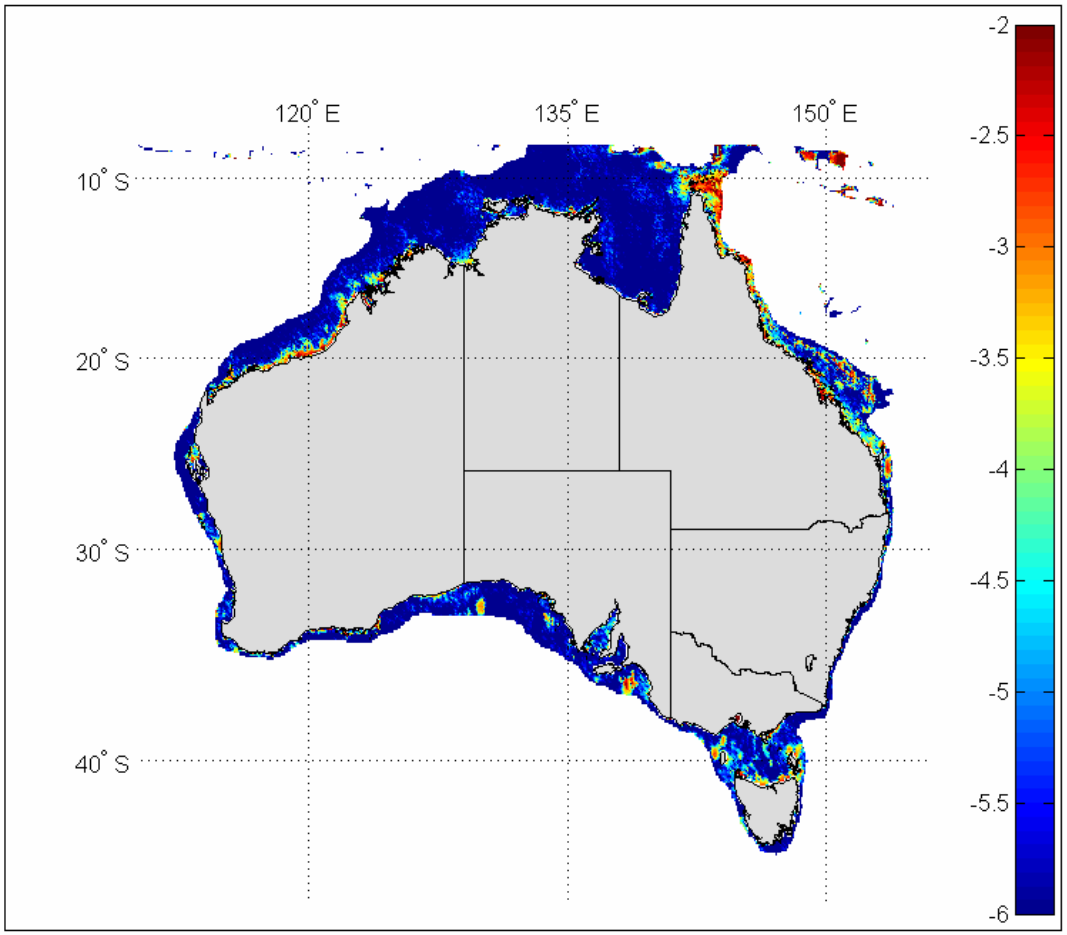

Figure A.4: Map showing logarithm of the modal bed shear stress (Nm^{-2}) on the Australian shelf.

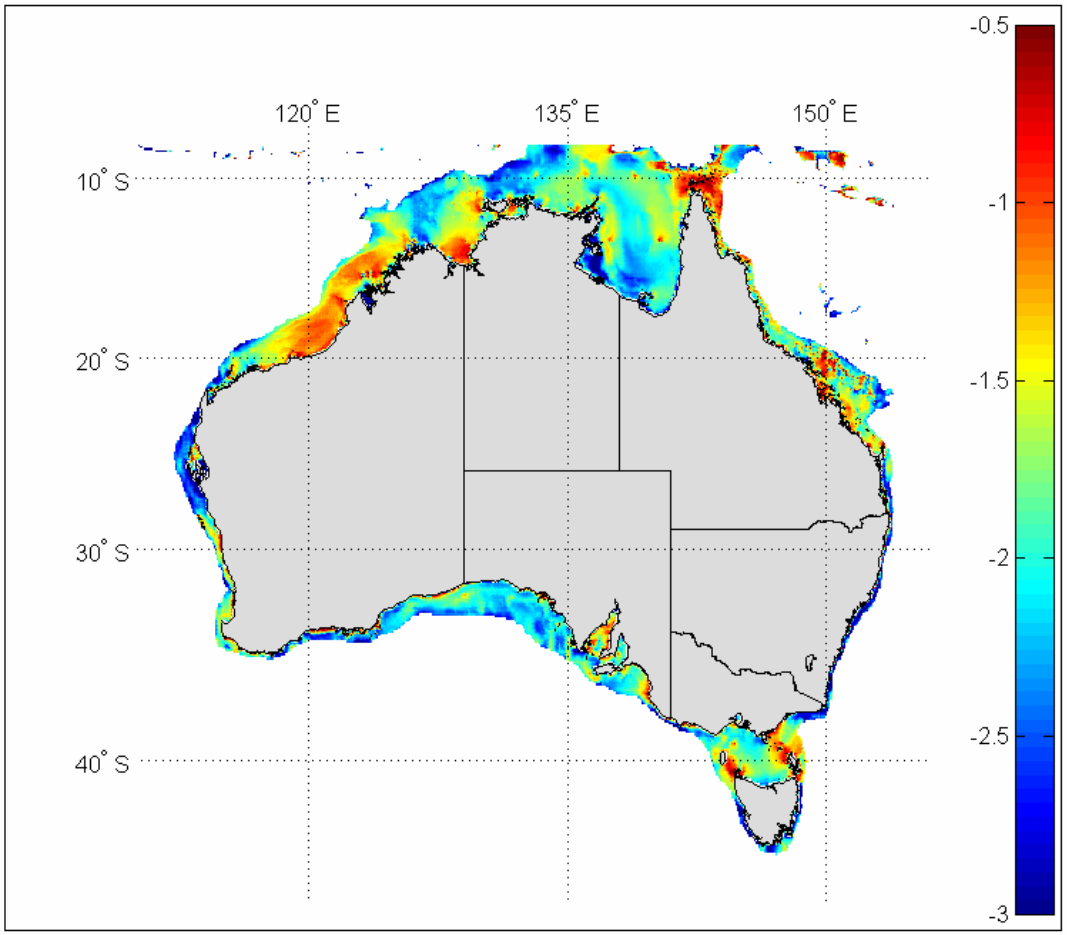

Figure A.5: Map showing logarithm of the 25th quartile bed shear stress (Nm^{-2}) on the Australian shelf.

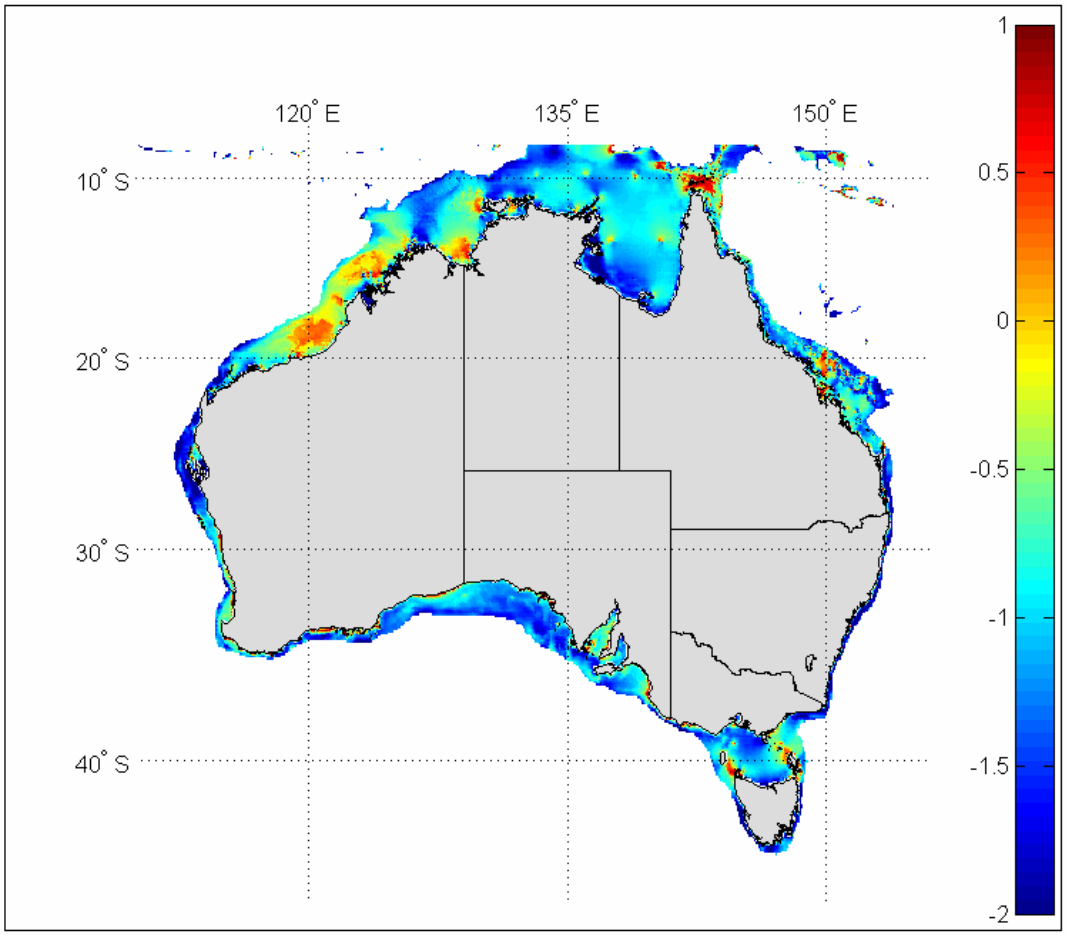

Figure A.6: Map showing logarithm of the 75th quartile bed shear stress (Nm^{-2}) on the Australian shelf.

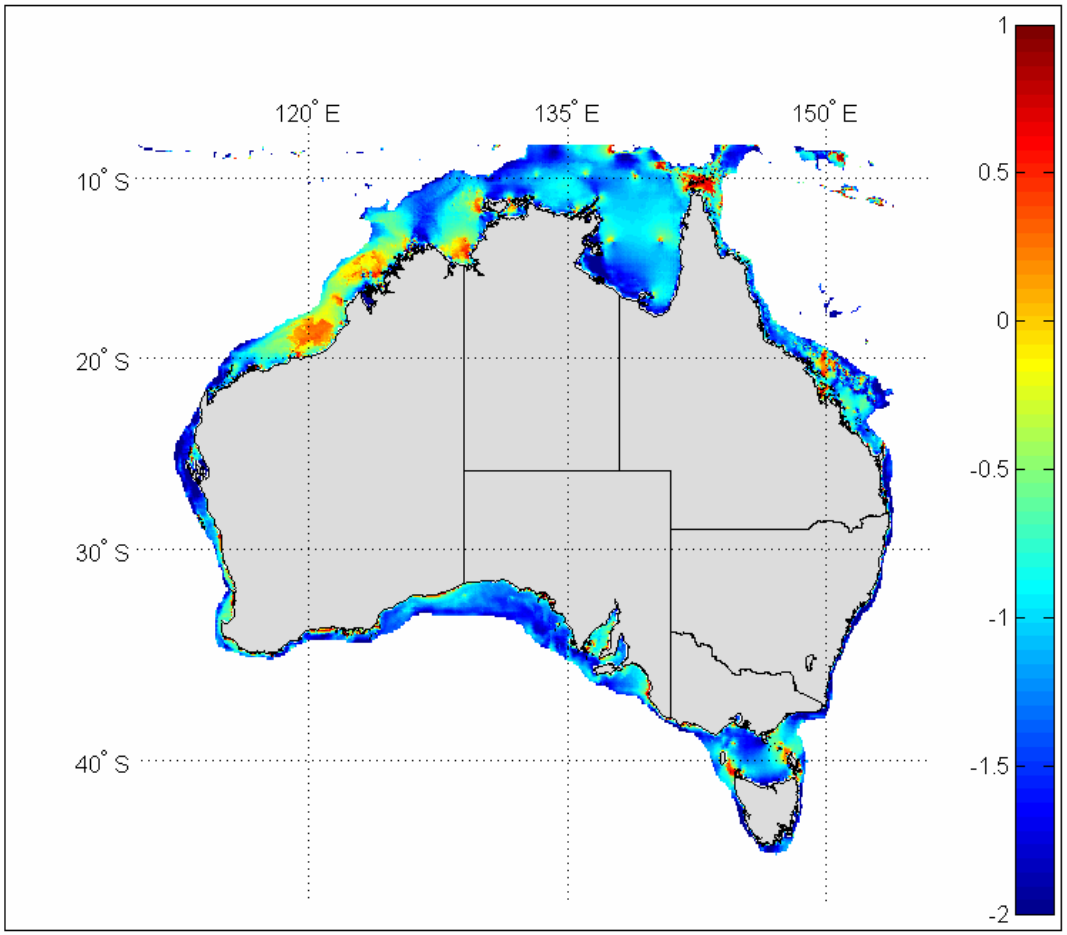

Figure A.7: Map showing logarithm of interquartile range bed shear stress (Nm^{-2}) on the Australian shelf.

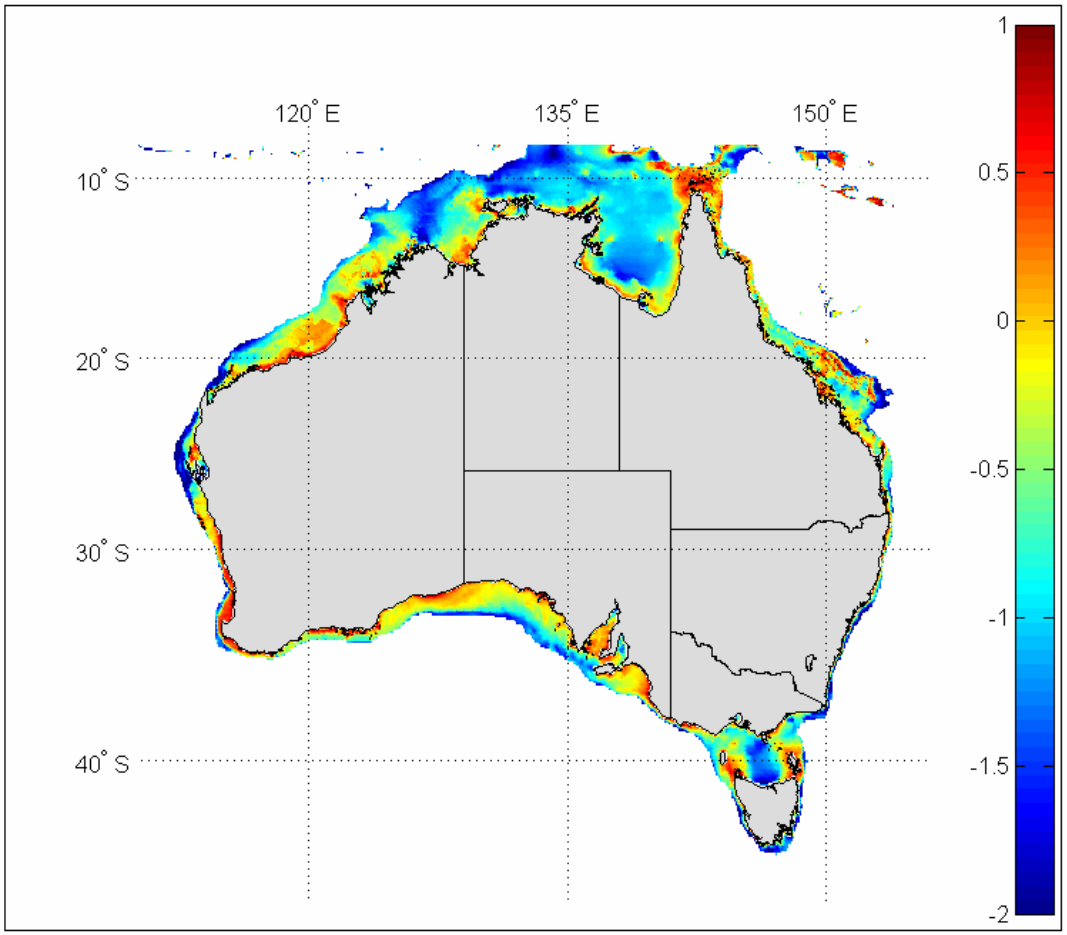

Figure A.8: Map showing logarithm of the standard deviation of bed shear stress (Nm^{-2}) on the Australian shelf.

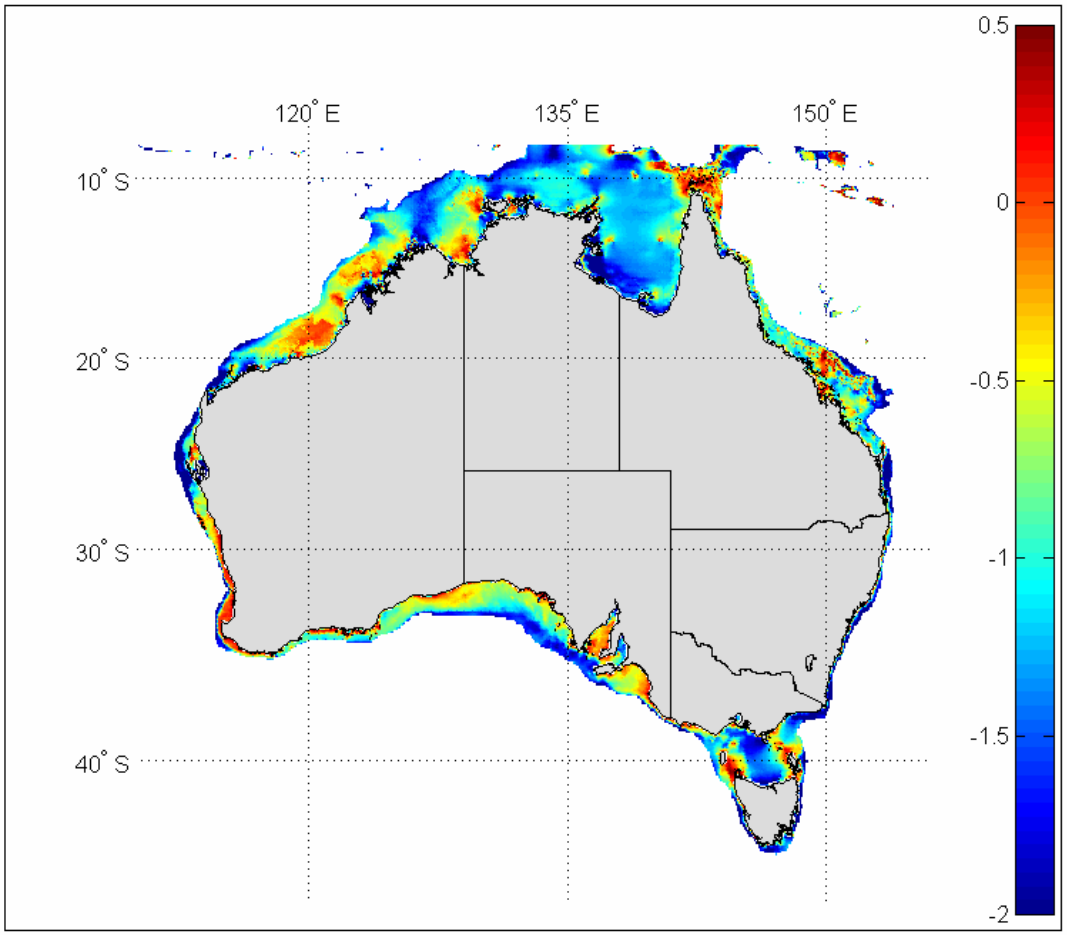

Figure A.9: Map showing logarithm of the mean daily standard deviation of bed shear stress (Nm^{-2}) on the Australian shelf.

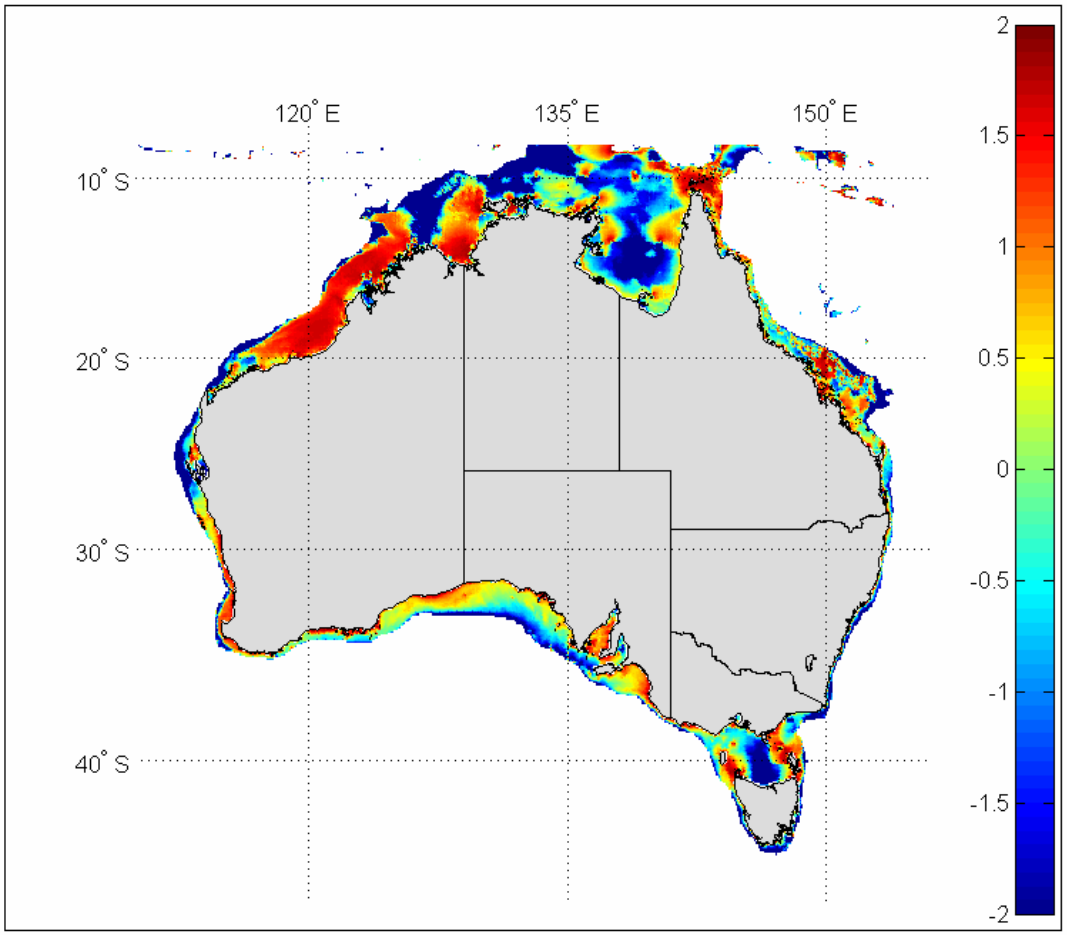

Figure A.10: Map showing logarithm of the percentage-time the bed shear stress exceeds 0.4 Pa on the Australian shelf.

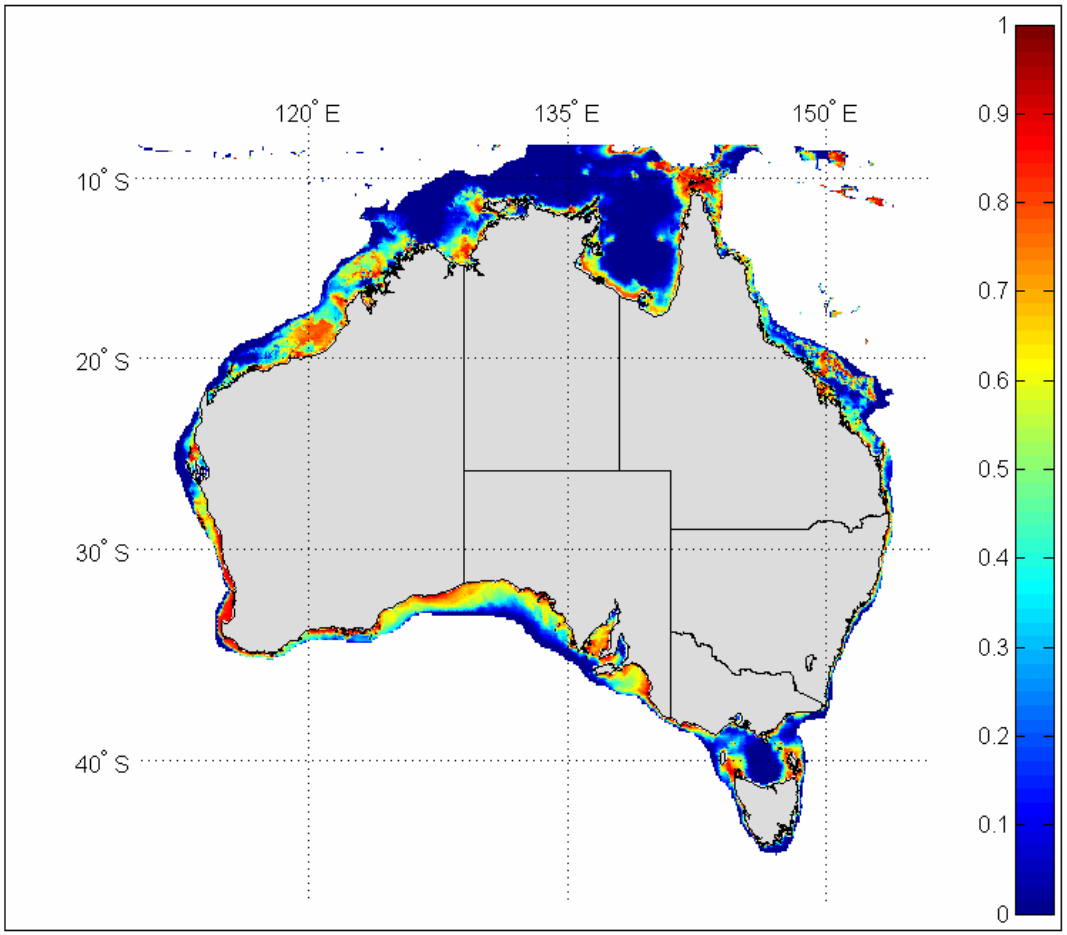

Figure A.11: Map showing logarithm of the parameter *R* (calculated using Equation 4.1) on the Australian shelf.

Appendix B

Maps of possible surrogates for ecological disturbance on the Australian shelf

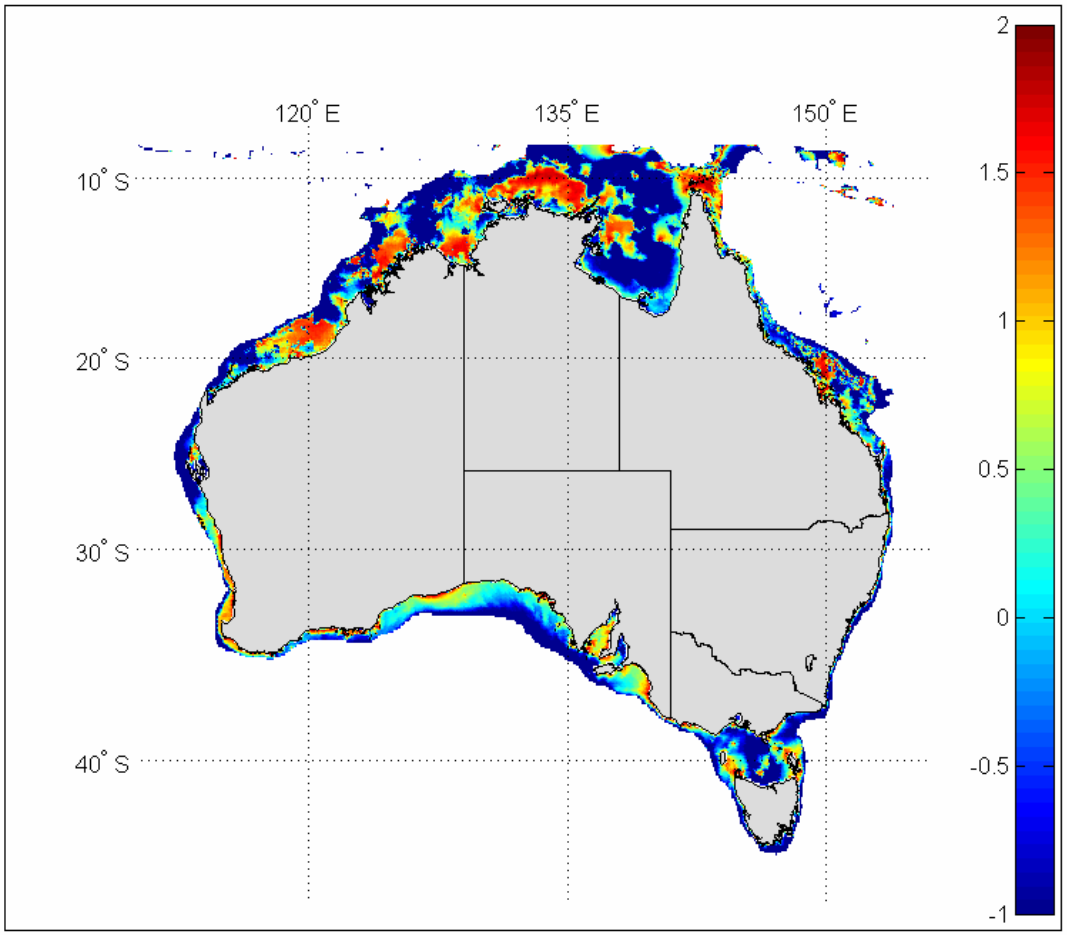

Figure B.1: Map showing logarithm of the percentage of time that the Shield's parameter exceeds 0.25 on the Australian shelf.

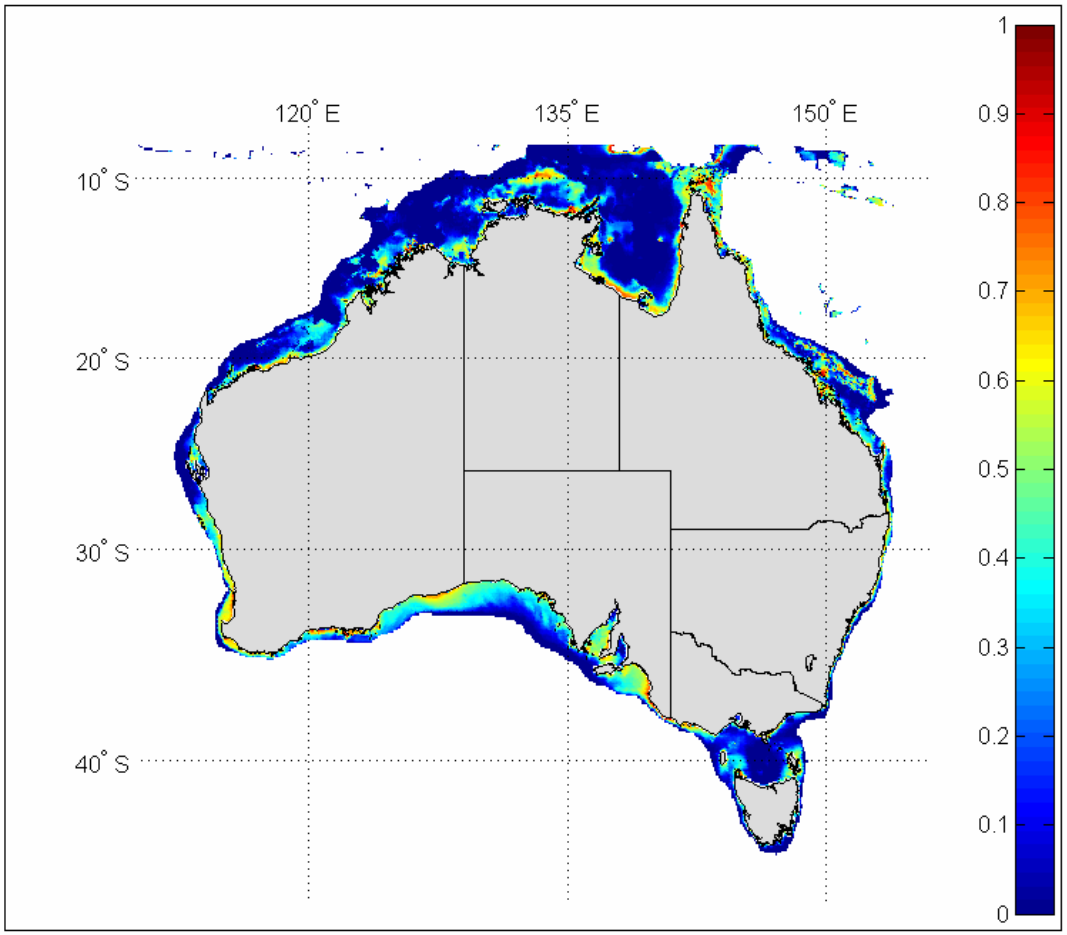

Figure B.2: Map showing logarithm of the parameter *R* (calculated using Equation 5.2) on the Australian shelf.

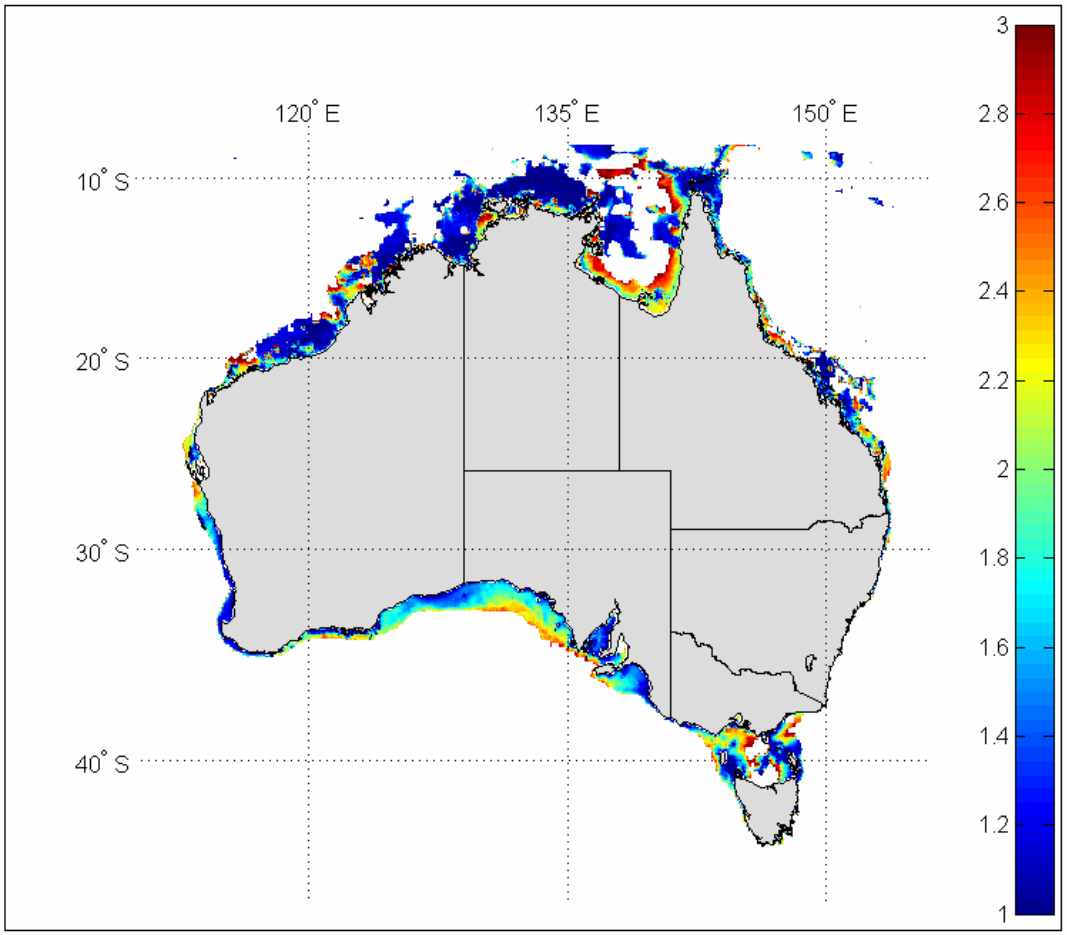

Figure B.3: Map showing logarithm of number of days between events where the Shields parameter exceeded 0.25 on the Australian shelf.

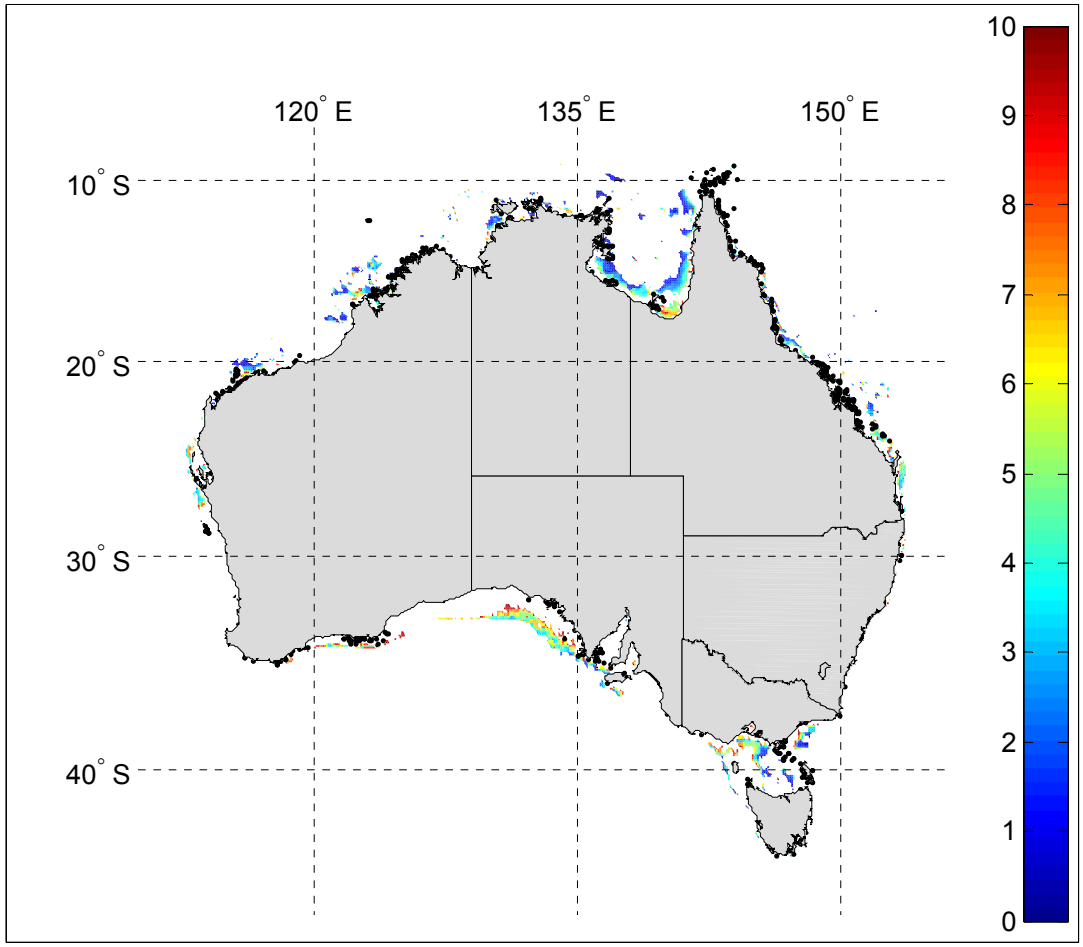

Figure B.4: Map showing the ecological disturbance (*ED*) index on the Australian shelf. Note *FA*=1 was used in the calculation (see Eq. 5.1). White areas apply to values of ED greater than 10 and less than 0.2.